



BARC0141: Built Environment Dissertation

Functionally graded 3D printing toolpaths

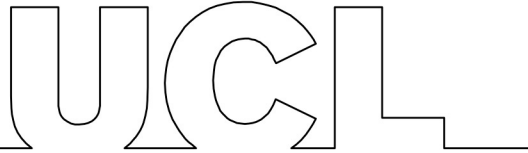
by

Julius Überall

11. September 2022

Dissertation submitted in part fulfilment of the
Degree of Master MSc Architectural Computation

Bartlett School of Architecture
University College London



MSc Architecture Computation Dissertation Submission Form

A signed and dated copy of the following MUST be inserted after the title page of your dissertation. If you fail to submit this statement duly signed and dated, your submission will not be accepted for marking.

1. DECLARATION OF AUTHORSHIP

I confirm that I have read and understood the guidelines on plagiarism, that I understand the meaning of plagiarism and that I may be penalised for submitting work that has been plagiarised.

I certify that the work submitted is my own and that it has been also submitted electronically and that this can be checked detection service, Turnitin®.

I declare that all material presented in the accompanying work is entirely my own work except where explicitly and individually indicated and that all sources used in its preparation and all quotations are clearly cited.

Should this statement prove to be untrue, I recognise the right of the Board of Examiners to recommend what action should be taken in line with UCL's regulations.

2. COPYRIGHT

The copyright of this report remains with me as its author. However, I understand that a copy may be given to my funding body (alongside limited feedback on my academic performance). A copy may also be given to any organisation which has given me access to data and maps (if requested and if appropriate).

I also understand that a digital copy may be deposited in the UCL public access repository and copies may be available on the UCL library bookshelves.

Please write your initials in the box if you DO NOT want this report to be made available publicly either electronically or in hard copy.

Name: Julius Überall

Signed:

A handwritten signature in black ink, appearing to read 'Julius Überall'.

Date: 7. September 2022

Contents

Acknowledgement	3
Abstract	4
List of Figures	6
1 Research rationale	7
1.1 Challenge.....	7
1.2 Additive manufacturing in architecture.....	8
1.3 Functionally graded geometries	9
1.4 A sustainable, architectural, design framework driven by AM and FGD	10
2 Precedents	12
2.1 Large scale additive manufacturing in architecture	12
2.1.1 Toolpath design for material extrusion	13
2.1.2 Compression-only shells	14
2.1.3 Differential Toolpath Growth.....	15
2.2 Functionally Graded Design	16
2.2.1 Efficiency through grading properties	16
2.2.2 Functionally Graded Geometries.....	18
2.2.3 Design homogeneity and recyclability.....	19
2.3 Design-frameworks	20
2.3.1 CAD constraints: AM and FGD	20
2.3.2 Existing frameworks for AM and FGD	21
3 Functionally graded growth	23
3.1 Technology Stack	23
3.2 Graded differential growth (GDG)	23
3.3 3D printing toolpaths: NURBS-Curve GDG	25
3.3.1 Developable shells and point cloud seed	27
3.3.2 Functional UV gradients	28
3.3.3 Gradient remapped relaxation	32
3.3.4 Discretization: Interlocking panels	33
3.4 Architectural solids: Mesh GDG.....	36
3.4.1 Boundary shapes and functional 3D gradients	37

4 Evaluation	39
4.1 Contribution and discussion	39
4.2 Future Work	41
4.2.1 Functionally graded 3D printing toolpaths	41
4.2.2 Graded differential growth.....	42
5 Conclusion	43
5.1 Research summary	43
5.2 Conclusion	44
Bibliography	48

ACKNOWLEDGEMENTS

I want to value and stress the dedication, time commitment, and patience of my thesis supervisor Shajay Bhooshan, who guided me through my research and provided me with the necessary criticism.

Furthermore, I want to thank my technical supervisor Cesar Fragachan.

Additionally, I would like to express my sincerest appreciation for the German Academic Scholarship Foundation, which allowed me to pursue this degree by funding my postgraduate study. Without their support, inspiration, and belief, this study would not have been possible. Special thanks go to my advisors, Tanja Döller, Imke Thamm, and my confidential advisor Anja Vormann.

Finally, I want to thank my family, friends, and colleagues at the Bartlett, who stood confidently behind my work but were still curious enough to question it. They helped me to grow and inspired me throughout the year at the Bartlett.

ABSTRACT

Initiated by significant carbon emissions of accelerating urbanization (United Nations Environment Programme, 2021; United Nations, Department of Economic and Social Affairs, Population Division, 2022), there has been increasing interest in large-scale additive manufacturing (LSAM) and functionally graded design (FGD) in architecture. These innovations prove the potential to speed up, simplify and optimize design pipelines as well as manufacturing processes to contribute to a sustainable future (Ngo et al., 2018; Wong and Hernandez, 2012; Mahamood et al., 2012). Yet, conventional computer-aided design software frameworks lack facilitating and explicit modeling environments to utilize LSAM and FGD in the industry (Oxman et al., 2011; Hasanov et al., 2022; Bhooshan et al., 2018b,a). Furthermore, these domains get commonly separated because of their difference in design scale. This dissertation outlines a novel design framework combining LSAM and FGD. It introduces functionally graded, differential-grown, and discretized 3D toolpaths of compression-only shells for extrusion-based LSAM. The framework builds on this research's outlined algorithm for graded differential growth (GDG), introducing graded point relaxation. The dissertation also contains an overview of recent developments and design frameworks for LSAM and FGD in an architectural context.

Keywords: Functional grading, 3D printing toolpath design, Large-scale additive manufacturing, Differential growth, Compression-only shells

List of Figures

Figure 1	Global population growth & carbon emissions	7
Figure 2	Precedents: AM in architecture divided by material	8
Figure 3	Precedents: Functionally graded design in nature and architecture..	9
Figure 4	Functionally graded 3D printing toolpaths in architecture	10
Figure 5	Urschels' "Machine for building walls"	12
Figure 6	3DP toolpath design techniques	13
Figure 7	Striatus bridge.....	14
Figure 8	Shells in architecture.....	15
Figure 9	Thallus installation	16
Figure 10	Functionally graded design concept	17
Figure 11	Precedents: Functionally graded geometries.....	18
Figure 12	Difference between FGMs and FGGS.....	19
Figure 13	Influential design frameworks in architecture	20
Figure 14	Design software constraint for FGD and LSAM	21
Figure 15	Recent software developments for FGD and LSAM	22
Figure 16	Technology stack	23
Figure 17	Graded differential growth concept.....	24
Figure 18	Formula for graded point relaxation	24
Figure 19	GDG point cloud effect	25
Figure 20	GDG interface for NURBS curve	26
Figure 21	GDG concept applied to NURBS curve	26
Figure 22	Design framework for functionally graded 3DP toolpaths.....	27
Figure 23	GDCG: point cloud seed effect.....	28
Figure 24	GDCG: principle stress grading	29
Figure 25	GDCG: multi-layered grading	30
Figure 26	GDCG: gradient calculation approaches	31
Figure 27	GDCG: gradient contrast effect.....	32
Figure 28	GDCG: gradient remapped relaxation	33
Figure 29	GDCG: discretization.....	34
Figure 30	GDCG: discretization techniques	34
Figure 31	GDCG: dynamic updating gradient map	35

Figure 32	GDG interface for mesh	36
Figure 33	GDG concept applied to mesh	36
Figure 34	Design framework for functionally graded solids.....	37
Figure 35	GDMG: architectural application.....	38
Figure 36	GDMG: 3D gradient map.....	38
Figure 37	Effect of GDCG and GDMG on architectural components.....	39
Figure 38	GDCG design framework.....	40
Figure 39	GDCG: concept rendering	41

1. RESEARCH RATIONALE

Architecture in the 21st century needs design innovation — it constrains itself with frameworks that address outdated needs (Oxman et al., 2011; Hasanov et al., 2022; Bhooshan et al., 2018a). Manual analysis and human crafting still dominate contemporary design thinking and shape Computer-Aided Design (CAD) in architecture which in its purest form ignores any real-world feedback (Mitchell, 1990). As a result, the consumption of materials is too high, inefficient, and unsustainable. In 2021, the building and construction industry contributed approximately 37% to the global CO₂ emission, 10% from the building construction alone (United Nations Environment Programme, 2021). Additionally, urbanization is globally accelerating undistributed due to significant population growth in low-income countries (United Nations, Department of Economic and Social Affairs, Population Division, 2022; Müller and Harnisch, 2008), creating ecologic and economic urbanization centers in challenging regions. Consequently, the lack of resources combined with current frameworks forces a global trend of unsustainable, inefficient, and material-consuming architectural design.

1.1. CHALLENGE

With increasing urbanization, architectural design needs to be optimized, lowering the need for building materials, accelerating as well as facilitating construction, and simplifying advanced design frameworks to aim for a sustainable future (Figure 1). However, the spatial quality and comfort should be unaffected and possibly improved.

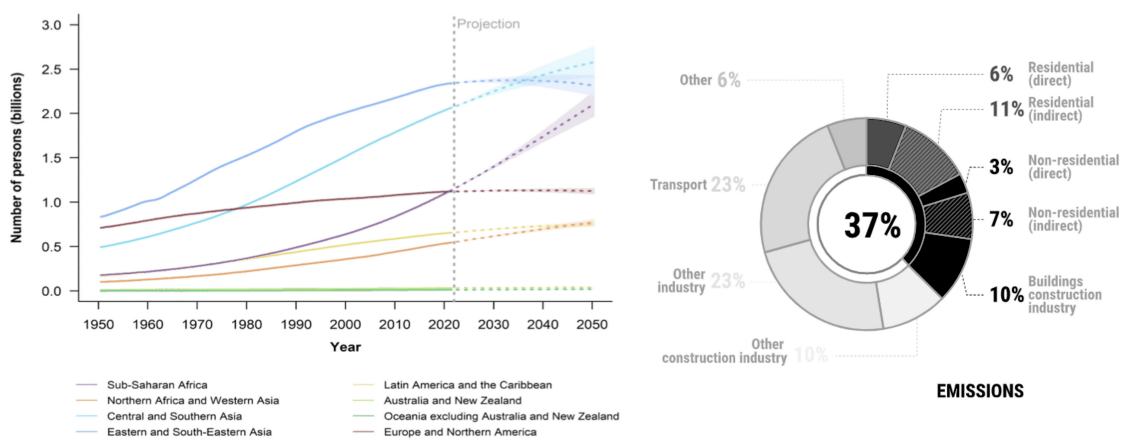


Figure 1: Left - Population estimates, 1950–2022, and projections with 95% prediction intervals, 2022–2050, by region; Right - Buildings and construction's share of global energy-related CO₂ emissions, 2020. Images and captions from, Left - (United Nations, Department of Economic and Social Affairs, Population Division, 2022), Right - (United Nations Environment Programme, 2021)

1.2. ADDITIVE MANUFACTURING IN ARCHITECTURE

Additive manufacturing (AM) has received significant interdisciplinary research attention in the last decade, reimagining fabrication by lowering costs, materials, and fabrication time while increasing accuracy as well as complexity (Ngo et al., 2018; Wong and Hernandez, 2012). In 2017 only 3% of the global applications of the AM industry were considered architectural (Campbell et al., 2017). Even though the uptake of AM in the building and construction industry is slow, it embodies the unprecedented potential to accelerate and simplify construction processes while utilizing minimal material and introducing design freedom. It eliminates formwork, automates construction, increases safety and health conditions for workers, and enables mass customization. It shows the potential to bridge the gap between design optimization and manufacturability to create a more efficient, accelerated, and sustainable urbanization.

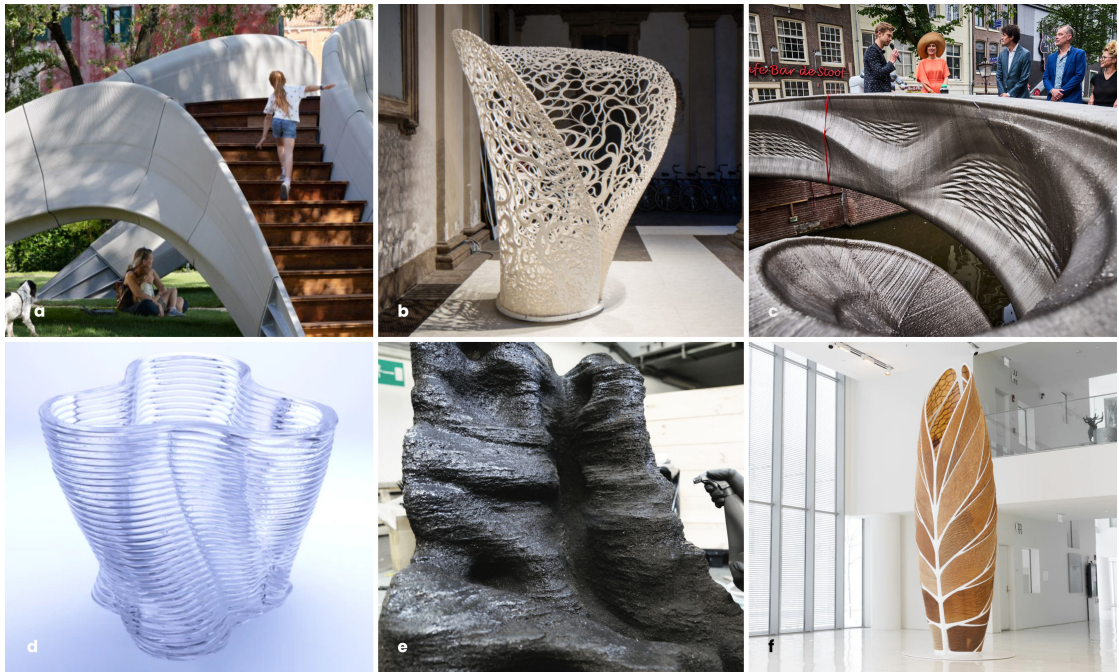


Figure 2: Additive manufacturing in architecture divide by material: a - Concrete, b - Plastic, c - Metal, d - Glass, e - Soil, f - Chitosan(Chitin). Images from, a - (ZHACODE et al., 2021), b - (ZHACODE, 2017), c - (MX3D, 2021), d - (Klein et al., 2015), e - (Mitterberger and Derme, 2020), f - (Duro-Royo et al., 2018)

AM in architecture opened up an entire research domain resulting in predominantly material-driven studies with concrete (Bhooshan et al., 2018a), plastics (ZHACODE, 2017), metals (MX3D, 2021), glass (Klein et al., 2015), soil (Mitterberger and Derme, 2020), chitin (Duro-Royo et al., 2018), and many more (Figure 2). However, large-scale AM is still constrained and not fully integrated into conventional workflows within the Architecture Engineering and Construction (AEC) industry due to a lack of research in explicit architectural geometry (AG) modeling for AM (Bhooshan et al., 2018b). The

rife approach in architecture to develop top-down designs, unaware of their fabrication technique, is still dominating the architectural industry and significantly barring the uptake of large-scale AM. This design-thinking causes many printing failures and poses, in general, a too big risk for architecture offices and clients to utilize AM in large-scale projects. Indeed, large-scale AM in architecture requires domain-specific architectural geometry, a novel design language in architecture. Yet it is indispensable to reimagine CAD to provide a clear framework for this new design paradigm to get considered in the industry and to lower carbon emissions globally.

1.3. FUNCTIONALLY GRADED GEOMETRIES

Functionally Graded Geometries (FGGs) caught many of AM's attention by representing high-performance designs that could only get achieved through AM. They constitute another promising domain for sustainable architecture, extending architectural geometry modeling and eliminating the need for material composites in multi-demanding conditions.

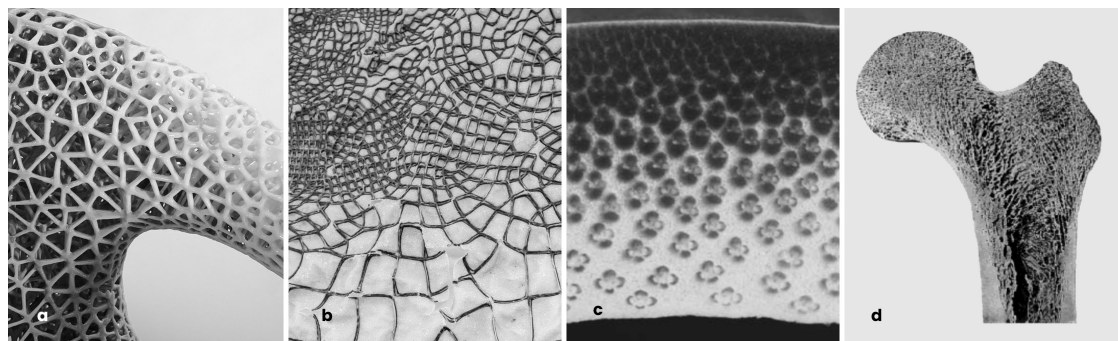


Figure 3: Functionally Graded Geometries in architecture and nature: a - Detail of durotaxis chair, b - Detail of aguahoja pavillion, c - Section of bamboo, d - Section of bone. Images from, a - (SynthesisDesign+Architecture and Stratasys, 2014), b - (Duro-Royo et al., 2018), c - (Obataya et al., 2007), d - (Simancik, 1999)

FGGs belong to the domain of Functionally Graded Design (FGD), which Japan's Science and Technology Agency first introduced in the 1980s in an aerospace context (Shinohara, 2013) and which received an ever-since increasing interdisciplinary research attention (Gupta and Talha, 2015; Mahamood et al., 2012).

FGGs are conceptually based on nature, one example being mimicking the extracellular matrix of human bones, which reinforces the bone's structure with minimal material by grading trabecular tissue (Wolff, 2012)(Figure 3.d). They generally re-model boundary representations (BRep)s on a mesoscopic, geometric level through graded, discretized structures. The resulting geometry gradients form heterogeneous material properties, enhance the use for multi-demanding conditions, and maximize the efficiency of components. Nevertheless, FGGs apply to homogeneous, single material designs and heterogeneous, multi-material designs, which often blur the line between them and Functionally Graded

Materials (FGMs) (Duro-Royo et al., 2018; SynthesisDesign+Architecture and Stratasys, 2014). Rather than geometry, FGMs functionally distribute two or more materials with desired physical features to develop such gradients (Shinohara, 2013). However, the material homogeneity of FGGs represents a desirable property for global application in large-scale AM for sustainable urbanization because of their high recyclability, especially in low-income countries (de Mello Soares et al., 2022).

FGGs represent a design optimization modeling technique that overcomes the need for binders and multi-material designs and increases its component durability, structural efficiency, and recyclability. In addition, it lowers the amount of material by functionally distributing its density in gradients to fulfill the multi-demand as minimal as possible.

1.4. A SUSTAINABLE, ARCHITECTURAL, DESIGN FRAMEWORK DRIVEN BY AM AND FGD

Contemporary CAD frameworks constrain AM and FGD through unexplicit architectural geometry modeling environments and geometry data structures like BRepS or meshes. Hence, it prevents the uptake of these novel concepts, especially in architecture, and forces material-consuming, inefficient, and unsustainable designs or time-consuming, expensive, and custom-developed workflows. However, with increasing urbanization pre-dominantly in low-income countries, a globally applicable design framework needs to be set up, increasing the construction efficiency, ecology, and economy to have a long-lasting, sustainable impact.

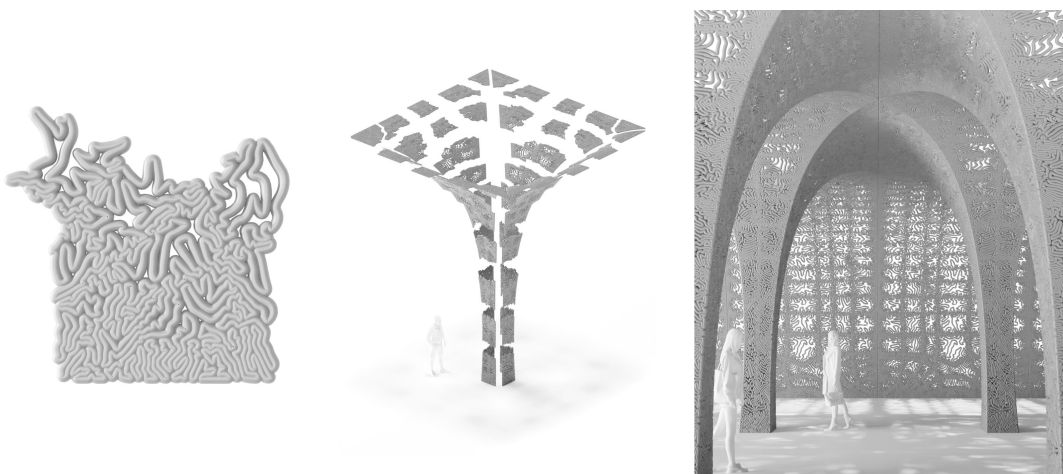


Figure 4: Concept: Functionally graded, differential grown, and discretized toolpaths for large scale additive manufacturing in architecture working in compression.

This research investigates the intersection of large-scale additive manufacturing (LSAM) and functionally graded geometries (FGGs) to bridge computational design and manufacturing to lower carbon emissions in architecture by diminishing material

waste and accelerating construction (Figure 4). The research aims to develop a computational design framework utilizing and cross-connecting large-scale AM and FGGs to extend CAD and ultimately unlock new architectural geometry to contribute to a sustainable global AEC industry. The research concentrates on the following fields:

- graded differential growth as a modeling technique for heterogeneous and anisotropic geometry
- development of a flexible and autonomous computational design framework, facilitating architectural geometry modeling for extrusion-based large-scale AM in architecture
- functionally graded toolpath design for increased structural performance and architectural quality through optimized material exposure - tectonism in large-scale AM (Schumacher, 2017)
- toolpath discretization for large-scale AM through differential grown, interlocking panels
- compression-only shellular toolpath design

2. PRECEDENTS

2.1. LARGE SCALE ADDITIVE MANUFACTURING IN ARCHITECTURE

Automated, large-scale fabrication is a desired concept in the AEC industry that professionals have researched for decades. Vastly accelerating construction while reducing costs, human resources, and materials have been the essential motivations ever since. Already 40 years before world-changing additive manufacturing technologies like Fused Deposition Modeling (Crump, 1992) or Stereolithography (Hull, 1984) got invented and patented, William E. Urschel pioneered large-scale additive manufacturing in architecture. Urschel used the patented "Machine for building walls" to construct three full-scale architectural prototypes on the site of Urschel Laboratories Inc. in Valparaiso, the United States (Mehl, 2021) (Figure 5). The machine used a funnel to manually fill lean concrete and a roller to compress it to printed layers of approximately 18cm height while moving radial around a central z-axis. The technique also allowed Non-planar AM by rotating the machine, which enabled the construction of dome-like overhangs, working in compression (Figure 5.b and .d).

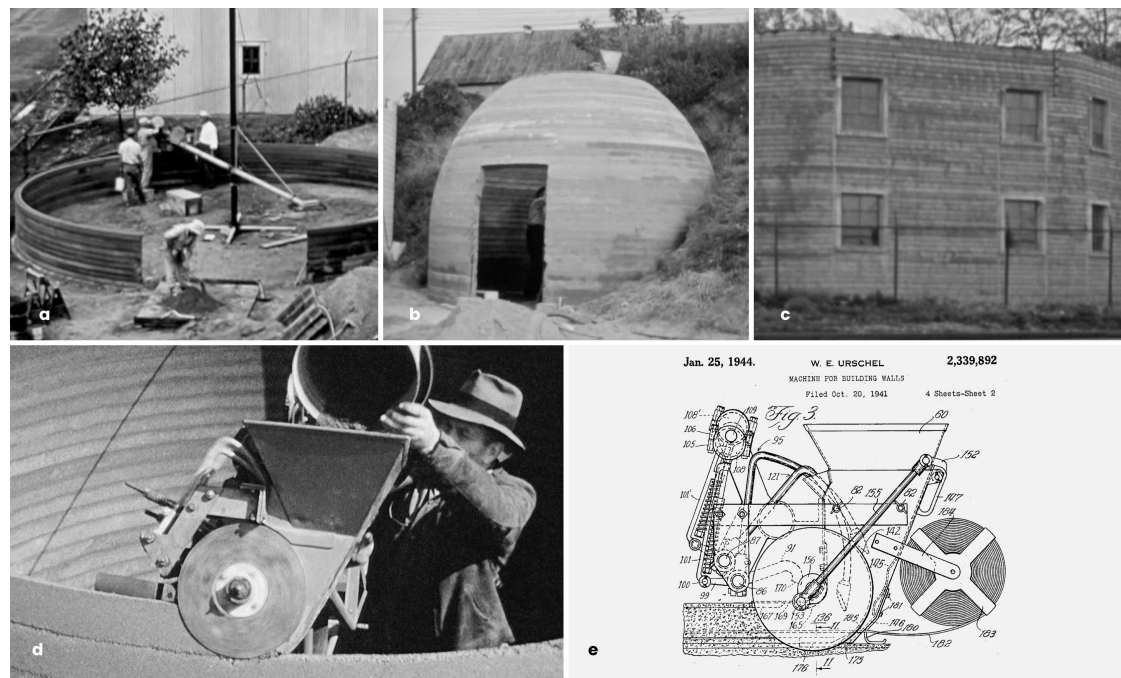


Figure 5: Urschel's "Machine for building walls": a - Prototype #1, b - Prototype #2, c - Prototype #3, d - Machine, e - Patent. Images from a-d (Mehl, 2021) and e (Urschel, 1944)

Nevertheless, AM finally caught interdisciplinary attention and research in the 1970 and 80s with the invention of STL technology, a rapid prototyping technique based on photochemical processes to harden photosensitive liquids with light (Hull, 1984). However, only FDM or so-called material extrusion in the 1990s made AM applicable for large-scale

fabrication in architecture (Crump, 1992). It introduced robotic nozzle printing, which allocates material to pre-defined 3D toolpaths in space, a concept first mentioned in 1945 (Leinster, 1945). Today it is considered one of the most widely used AM techniques worldwide (Mohamed et al., 2022).

2.1.1. Toolpath design for material extrusion

With the increasing popularity of AM in multiple domains, its front-end gained significant importance due to its useability and deployment. The conventional workflow for this is, until today, a so-called slicer, which provides a software framework to translate CAD designs into executable toolpaths (Dolenc and Mäkelä, 1994). Commonly these frameworks create planar toolpaths by slicing boundary representations (BRep) or meshes parallel to its XY plane without further consideration of the geometry topology (Figure 6.a). It is a loss of information from a geometrical standpoint and still the same difficulty from a manufacturing standpoint. However, planar toolpaths work for planar objects (Wolfs et al., 2019) but significantly constrain conventional, curved shapes in their printability and structural efficiency. This correlates with the brick masonry-like behavior of printed concrete layers and their dependency on force flow-oriented, perpendicular compression (Bhooshan et al., 2018b,a).

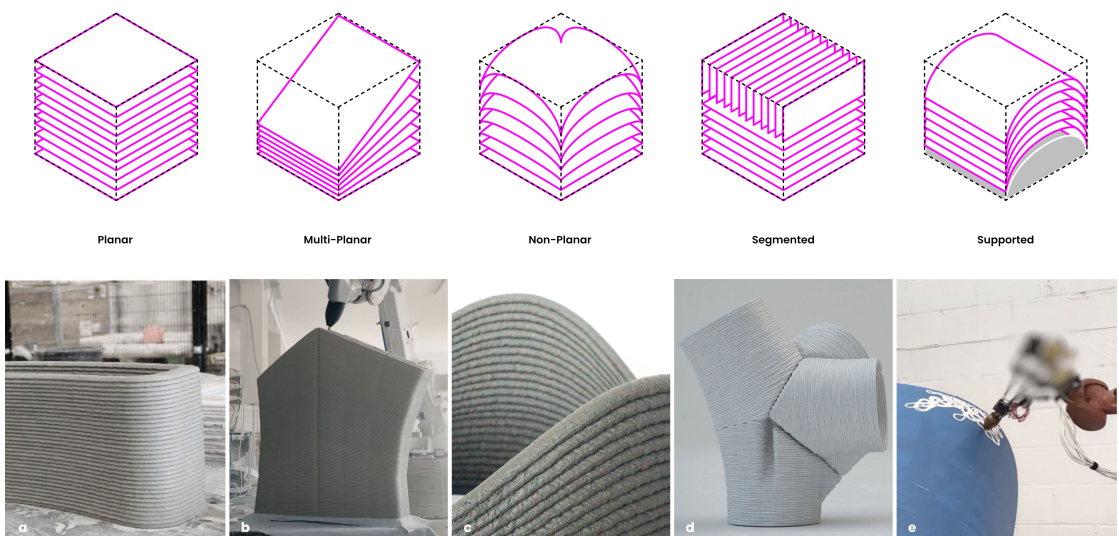


Figure 6: Material extrusion toolpath design concepts: Planar, Multi-Planar, Non-Planar, Segmented, Supported. Images from, a - (Wolfs et al., 2019), b - (ZHACODE et al., 2021), c - (Anton et al., 2019), d - (Bhooshan et al., 2018a), e - (ZHACODE, 2017)

Toolpath design has recently received much research, explicitly focusing on the applicability of large-scale AM in architecture to bridge the gap between design, printing execution, and structural efficiency. Studies with multi-planar (ZHACODE et al., 2021), non-planar (Anton et al., 2019), segmented (Bhooshan et al., 2018a), and supported (ZHACODE, 2017) printing paths (Figure 6), contributed to unprecedented large-scale

additive manufactured projects in architecture during the last years. They pioneered new architectural geometry, a design language in architecture driven by 3DP.



Figure 7: Striatus: Multi-planar 3D concrete printed masonry working through compression-only shells. Images from (ZHACODE et al., 2021)

The Striatus bridge by ZHACODE et al. (2021) constitutes an architectural novelty, proofing the ecological, economic, and tectonic qualities of AM architecture (Figure 7). Taking advantage of the brick masonry-like behavior of 3D concrete printed layers (Bhooshan et al., 2018b,a) from the beginning of the design process, the bridge creates a high-performance shellular structure out of 53 unreinforced, discretized, and multi-planar printed concrete blocks, working in compression only. The bridge eliminated the complex formworks of multiple unique blocks, the need for binder to connect the blocks, the construction and dissemble time, and the carbon footprint by using AM technologies and explicit architectural geometry. It showcases that an explicit design framework is needed to execute large-scale AM projects in architecture and diminish carbon emissions in the AEC industry.

2.1.2. Compression-only shells

Shell structures are lightweight, thin sectioned, and self-supporting geometries of structural high-performance defined and characterized by curvature. Throughout architectural history, they got applied to large-scale constructions and shaped structural engineering in architecture. However, during the last century, shells lost popularity in construction due to their complexity, constituted through their expensive formworks and challenging analysis and modeling (Tang, 2015).

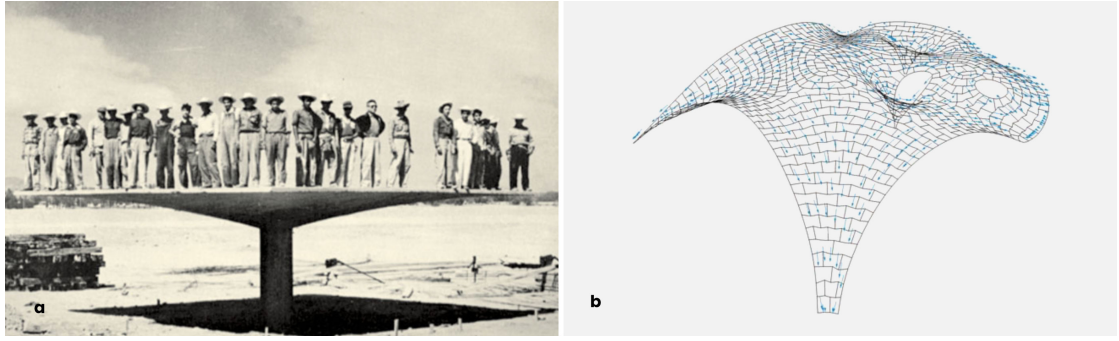


Figure 8: Shell structures historic and contemporary usecase: a - Prototype umbrella by Félix Candela (Las Aduanas, México, 1950), b - Unreinforced, discretized, stone-cut shell. Images from: a - (Scholzen et al., 2015), b - (Rippmann and Block, 2013)

Compression-only shells constitute an architectural geometry tailored for materials, techniques, and discretized shapes characterized by compression strength (Rippmann and Block, 2013). The Striatus bridge heavily relies on those, enabling the use of unreinforced and 3D-printed concrete, characterized by its compression through its material properties and printing layer behavior (Bhooshan et al., 2018b).

Concrete is globally the second most used material after water and, particularly in architecture, the most utilized building material as of today (Barcelo et al., 2014; Wangler et al., 2016). Therefore, the AEC industry and its architectural design frameworks must adopt and support architectural geometry modeling for concrete, especially for unreinforced, 3D-printed concrete, through compression-only shells to let large-scale AM take off in the global industry.

2.1.3. Differential Toolpath Growth

Differential Growth (DG) belongs to the domain of morphogenesis, developing complex and high-performance 3D geometry in plants like leaves and flowers (Huang et al., 2018). For decades humans studied the rich expertise of morphogenesis in form (Rosenkrantz and Louis-Rosenberg, 2014; Haeckel, 1899), optimization (Bendsøe and Kikuchi, 1988), and patterns (Thompson, 1917; Prusinkiewicz and Lindenmayer, 1990; Dawkins, 1991; Stevens, 1974), contributing to innovations across disciplines. However, simplifying the biological concept of DG from 3D to 2D, for example, resulting in differential curve growth (DCG) (section 3.3), constitutes potential for optimized and form-found 3DP toolpaths for large-scale AM in architecture as shown in the Thallus installation by ZHACODE (2017).

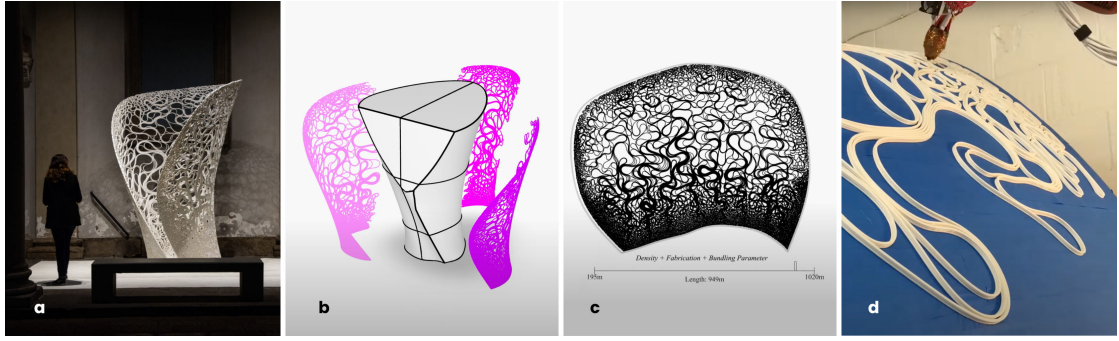


Figure 9: Thallus Installation: Differential grown, supported 3D printed toolpaths on ruled surface. Images from (ZHACODE, 2017)

The project introduced a bottom-up toolpath design framework, creating explicit curve geometry for 3DP by considering the topology of the base surface for generating the freeform curve. A flat, pre-defined toolpath-curve, UV projected onto a ruled surface, was grown differentially by relaxing and inserting control points, described similarly in section 3.3. The resulting toolpath showcases the use of a boundary and z-axis density gradient, ensuring structural stability. Nevertheless, the gradient is not uniform and indicates some randomness, represented by non-linear density anomalies in the center of the surface (Figure 9.c). Additionally, for architectural variations of the curve pattern, ZHACODE (2017) explored the relation between start-curve and grown-curve, varying in densities and structural performance and integrating some user-defined constraints in the toolpath design framework. However, the differential-grown toolpath got printed supported onto a curved formwork with premium polylactide plastics (PLA), and discretized into three parts (Figure 9.b). It ensured accelerated assembly and disassembly on site and maximum transportation flexibility.

2.2. FUNCTIONALLY GRADED DESIGN

Functionally Graded Design (FGD) is a domain that focuses on creating property gradients to tailor components for unique and multifunctional conditions. The author divides the domain into Functionally Graded Materials (FGMs) and Functional Graded Geometries (FGGs). Functional grading is a concept derived from nature and occurring in the extracellular matrix of bones and bamboo to reinforce their structure with minimal material (Wolff, 2012; Simancik, 1999; Obataya et al., 2007)(Figure 3.c and .d).

2.2.1. Efficiency through grading properties

Japan's Science and Technology Agency created the domain of FGD in the 1980s by introducing FGMs to avoid losing the thermal protection tiles of its supersonic space plane, which was exposed to significant heat while transitioning through the earth's atmosphere

(Kawasaki and Watanabe, 1997; Shinohara, 2013). The inside-outside thermal difference of the plane was undistributed enough to result in thermal stress that outperformed the panel's joining strength. Therefore, the multifunctional demand was to develop a material that supplies a moderate climate inside while resisting the heat outside and providing a smooth transition from one condition to another, lowering thermal stress and avoiding separation. Until then, these panels were a composite material based on an additive approach. It created a multifunctional design by introducing new layers of a different material, which added a new property. The resulting fundamental problem was a feature matrix consisting of as many states as there were materials used in the composite. Therefore, the physical property behaved like a stairstep graph, jumping from one to another without any transition.

Functionally Graded Materials (FGMs) first introduced mixed property states within a volume. They extend the property matrix from a given set of conditions depending on the number of materials to a higher dimensional property space. They create new materials (defined through unique properties) by blending multiple. Consequently, FGMs can grade features within parts and accordingly influence the performance of solids (Figure 10).

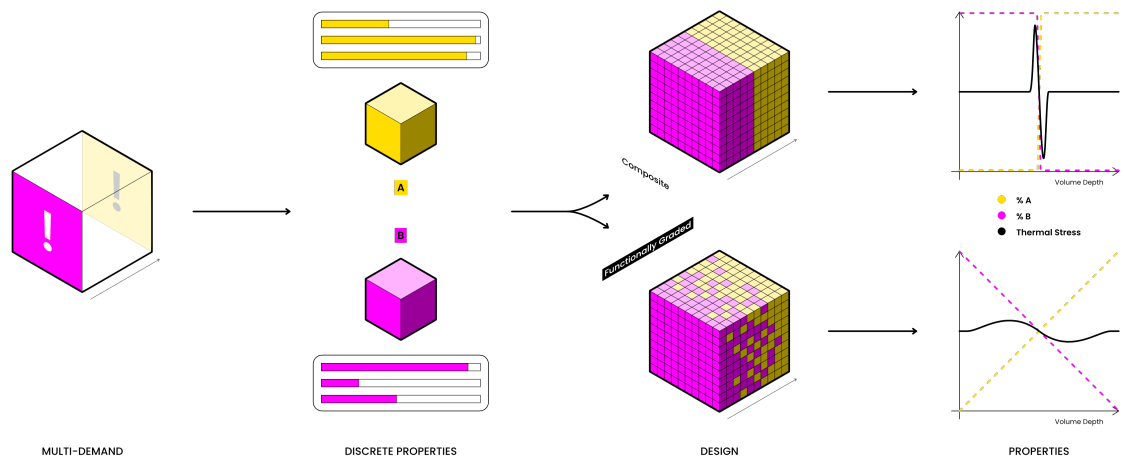


Figure 10: Solving multi-demands: A comparison of layered composite (top) and functionally graded materials (bottom) for thermal stress

FGMs created value in various domains, including next to aerospace, medicine, energy, defense, and optoelectronics. They were predominantly used to eliminate physical weaknesses in existing designs, appearing through layered composites to solve multifunctional demands. One example being bullet-proof vests at which FGMs could increase the ability to inhibit crack propagation and protect its carrier through feature gradients (Mahamood et al., 2012).

2.2.2. Functionally Graded Geometries

Functionally Graded Geometries (FGGs) are based on the concept of FGMs (Gibson and Ashby, 1997). They form the second of the two main branches within the domain of FGD.

Functionally Graded Geometries create feature gradients by altering the components' discrete cellular geometries. They make new materials by creating cells of different geometry, which result in other physical behavior, one example being decreased weight and strength through cell shapes with a loss of mass (Figure 12).

The Durotaxis Chair designed by SynthesisDesign+Architecture and Stratasys (2014) represents the concept of FGGs by altering the rigidity through local changes in the wire mesh's size, scale, and density. Similarly, Duro-Royo et al. (2018) created additive manufactured cell density gradients reacting to and harnessing hydration forces. Additionally, Niknam and Akbarzadeh (2019) explored the bending behavior of FGGs exposed to a thermo-mechanical load, synthesizing decreased or increased stiffness depending on the geometric family of cells (Figure 11).

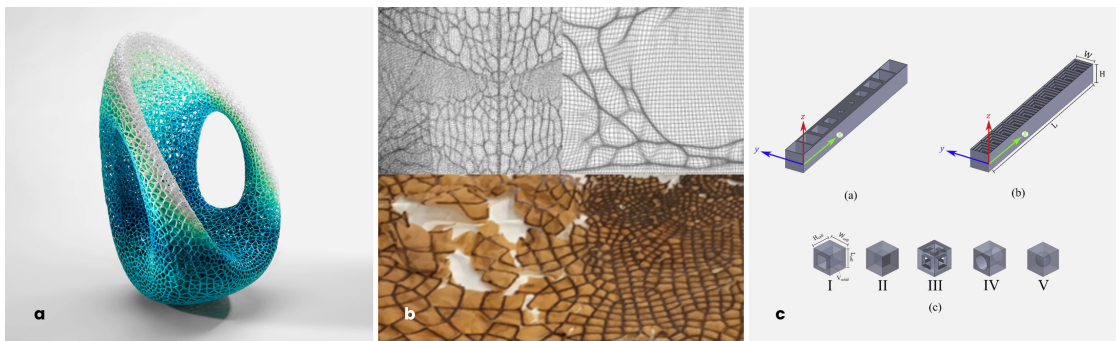


Figure 11: Functional Graded Geometries: a - Durotaxis Chair, b - Aguahoja Pavilion, c - Cellular beams. Images from: a - (SynthesisDesign+Architecture and Stratasys, 2014), b - (Duro-Royo et al., 2018), c - (Niknam and Akbarzadeh, 2019)

However, the main difference between FGMs and FGGs is the number of involved materials. FGMs have to have different materials that are getting mixed and graded through space to fulfill multi-demand, whereby FGGs only need one material. Therefore, FGMs must be heterogeneous, and FGGs can be homogenous materials (Figure 12). Alternatively, FGMs and FGGs could be interpreted as two different grading scales, altering the nano- or mesoscopic structure.

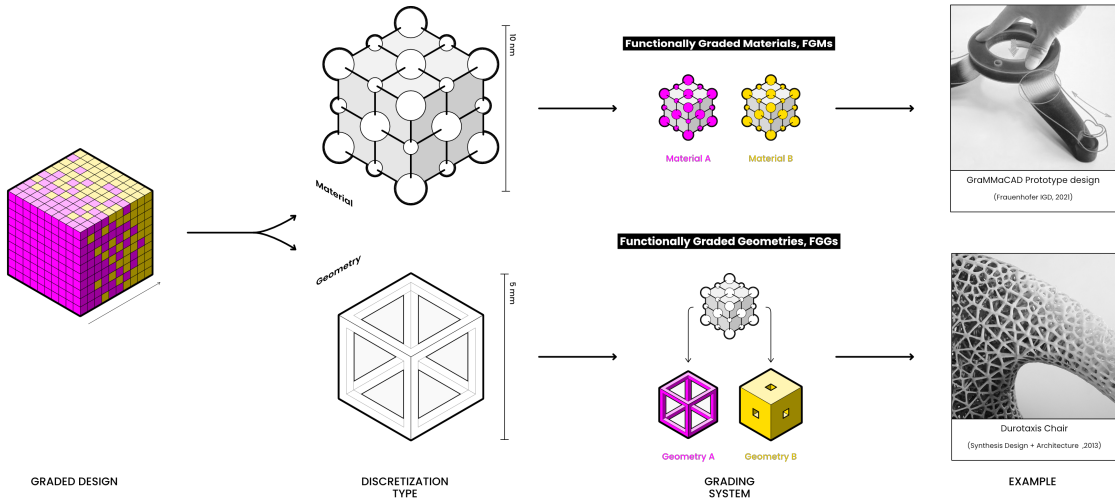


Figure 12: Functional Graded Design: A domain about grading physical features that divides into Functional Graded Materials (top) and Functional Graded Geometries (bottom). Images from: top - (IGD, 2021), bottom - (SynthesisDesign+Architecture and Stratasys, 2014)

2.2.3. Design homogeneity and recyclability

Recyclable architecture has recently gained much attention caused of AM's opportunity to fabricate recycled plastics and bio-degradable materials like shrimp shells (Duro-Royo et al., 2018) and soil (Mitterberger and Derme, 2020). However, material heterogeneity becomes especially relevant for the recycling industry and must be considered in a sustainable design framework for large-scale AM in architecture. Compared to FGMs that require multi-material additive manufacturing, FGGSs create graded, high-performance structures that are homogeneous and can be manufactured with single-material AM.

Multi-material multilayer plastics in packaging are already problematic for current recycling processes and block traditional waste management systems, which can not handle heterogeneous composites. With an increasing need for recyclable or bio-degradable waste to lower environmental pollution, trends in Europe already indicate the increased use of mono-material packages for recycling (de Mello Soares et al., 2022). Even though it is estimated that the development of advanced recycling systems for multi-material plastics will increase in the next decade, it is expected to happen predominantly in wealthy countries. Therefore, it does correlate with the growing population in low-income countries, which will create the most significant demand for architecture in the next century (chapter 1, Figure 1 left). Consequently, a design framework in the AEC industry tailored for AM to lower carbon emissions must consider the conditions within the global regions of demand, supporting recyclability and homogeneous materials.

2.3. DESIGN-FRAMEWORKS

Utilizing research and innovation across disciplines and ultimately in the industry to have a global impact requires straightforward and domain-tailored frameworks. Especially in architecture, pioneering projects often unveiled analog or digital workflows and design principles to incorporate new technologies and methods in future work. For example, in the 19th and 20th century, Antoni Gaudí form-found optimal, structural-aware arches using physical prototyping with catenaries informed by gravity to design the Sagrada Família. In the early 1970s, Frei Otto used soap film to explore and extract geometries of minimal surfaces to construct lightweight structures with minimal material like the Munich Olympic stadium. Moreover, in the 2020s ZHACODE et al. (2021) used large-scale additive manufactured concrete in combination with in compression working shell structures to construct the Striatus Bridge.

However, even though all of the mentioned projects above are based on concepts that were studied and discovered before (Figure 13), they had to reveal their unprecedented design frameworks, cross-connecting ideas and resulting in real-world architectural application and integration to prove and unify research and practice. All of the design frameworks are applied and existent until today.

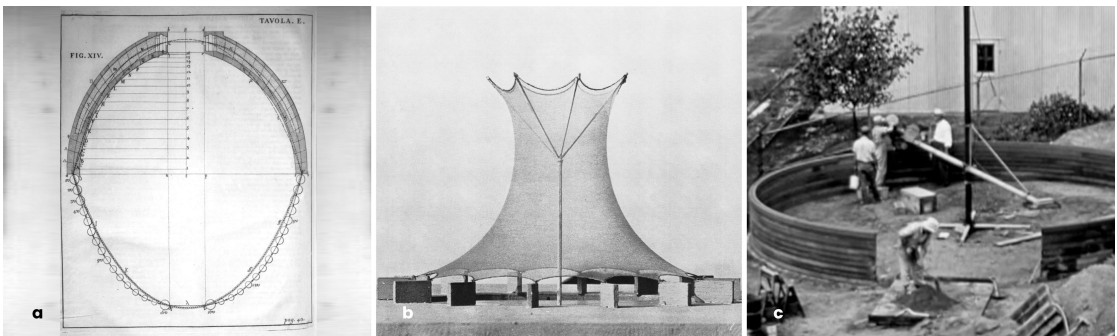


Figure 13: Influential design research concepts in the history of architecture that built the foundation of contemporary design frameworks : a - Catenary , b - Soap film , c - Large-scale AM with concrete. Images from: a - (Poleni and Poleni, 1748), b - (Yunis and Watkins, 2015), c - (Mehl, 2021)

2.3.1. CAD constraints: AM and FGD

Computer-Aided Design (CAD) is, since its development in the 1960s, the conventional interdisciplinary framework to create, analyze, and optimize designs. In architecture, it has dominated design thinking ever since. However, even though unlocking a new design paradigm back then, it constraints new research and innovations in the 21st century's AEC industry to fully take off and contribute to a sustainable future. Particularly in domains like AM and FGD.

CAD is restraining architecture, resulting in multiple, custom-developed software frame-

works disrupting a distributed and global incorporation of FGD and AM. One fundamental issue for FGD in CAD is the geometric concept of boundary representation (BRep) and meshes, which store no volumetric interior information of solids, representing only the envelope. Consequently, the computational structure of such geometries does not support heterogeneous property modeling through discretized cells or materials and constitutes an essential software gap for applying FGD and Multi-Material AM (Hasanov et al., 2022). CAD forces the assignment of materials and properties per solid (Oxman et al., 2011). On the other hand, CAD is too unconstrained in LSAM, as stated in subsection 2.1.1, and requires design frameworks to contain fabrication restraints for feasibility and explicit architectural geometry for 3DP (Bhooshan et al., 2018b,a)(Figure 14).

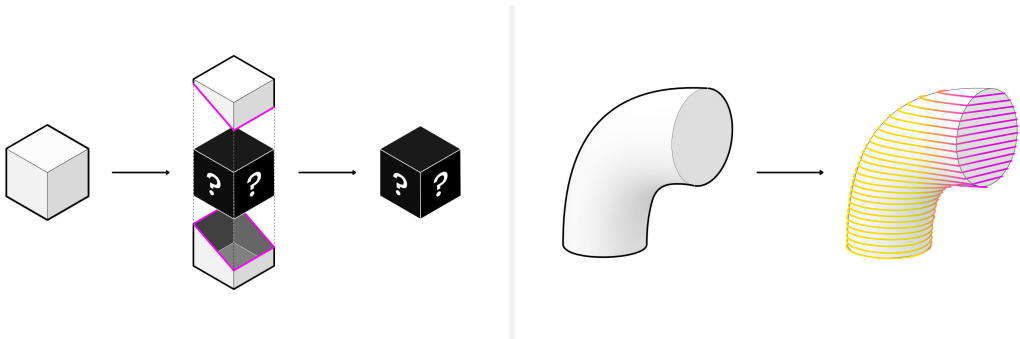


Figure 14: Design framework gaps for FGD and AM: left - FGD: BRep modeling without volumetric property information, right - Large-scale AM: Unconstraint toolpath generation and unexplicit architectural geometry modeling

The lack of CAD reacting to those needs leads to the undistributed current trend for large-scale AM or FGD designs to occur predominantly in research-heavy environments with the time, money, machinery, and knowledge required. Indeed the demand for software design tools to utilize the ecological values of LSAM and FGD in architectural design is increasing. The advantages of these technologies to diminish carbon emissions will only reveal if applied outside the labs, which desire widely applicable design frameworks.

2.3.2. Existing frameworks for AM and FGD

AiSync is a unique commercial, cloud-based software framework of the company AiBuild to slice, analyze, optimize and control 3D prints to utilize large-scale AM across disciplines (AiBuild, 2022). It got explicitly tailored for their custom large-scale 3D printer based on polymer extrusion, AiMaker. The application uses a real-time bi-directional data exchange with cameras and sensors to react and adjust the manufacturing process on the fly, changing the toolpath, threading rate, heat, orientation, and position to aim for successful and high-quality prints. Furthermore, the framework facilitates the execution and generation of advanced toolpath designs, like multi-planar and non-planar (subsection 2.1.1), taking full advantage of robotic deployment and unlocking structural efficiency

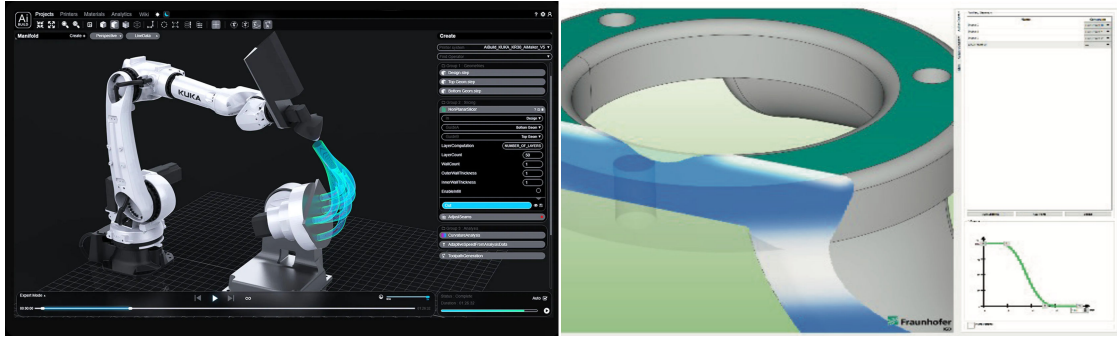


Figure 15: Design framework solutions for FGMs and AM: left - AM: AiSync, right - FGMs: GraMMaCAD. Images from: a - (AiBuild, 2022), b - (prostep ivip Association, 2021)

in printed parts.

Graded Multi-Material CAD (GraMMaCAD) is a unique commercial software tool to model graded material distribution for multi-material AM within CAD designs developed by Fraunhofer's Computer Graphics Research Department (IGD, 2021). It aims to establish FGMs within the industry by constructing an intuitive interface. There are three approaches to model the material gradients based on a CAD design: (1) Poly- or mesh faces will get materials assigned, creating a customizable gradient between them and inside the solid; (2) Custom-defined global planes act as gradient markers for the solid; (3) Discrete parts of the CAD model get assigned desired properties, resulting in an automated interpolation of the resulting to create a solid gradient fulfilling this unique multi-demand (Korner, 2020). GraMMaCAD stores the gradient through half-toned slices and manufactures the design with a VoxelPrint (prostep ivip Association, 2021).

3. FUNCTIONALLY GRADED GROWTH

3.1. TECHNOLOGY STACK

All implementations of this research are done within the environment of the commercial computer-aided design application software Rhinoceros 3D (RC) and its visual programming language, Grasshopper 3D (GH), on the operating system macOS. However, the actual algorithm itself represents a custom software extension in GH written in the programming language C#, using the application programming interface (API) of RC and GH.

The selected technological stack is in valuable proximity to computational design frameworks used in the architecture industry today and constitutes, therefore, the potential to be broadly applicable in practice.

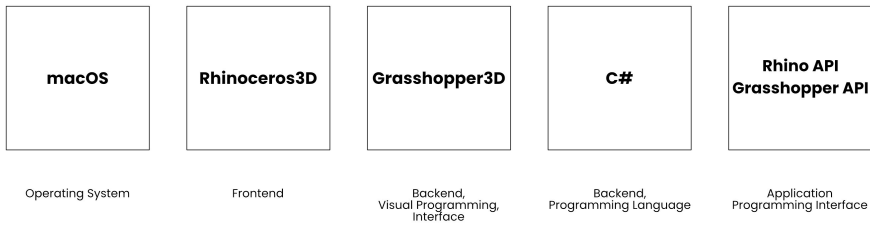


Figure 16: Research specific technology stack selected for implementing GDG

3.2. GRADED DIFFERENTIAL GROWTH (GDG)

Graded differential growth (GDG) is an emergent and deterministic algorithm in computational geometry based on the morphogenetic feature of plant cells called differential growth (Huang et al., 2018). It correlates and extends the computational work of Menges and Nguyen (2018) and ZHACODE (2017).

The underlying system is a list of vectors individually representing points and collectively representing a point cloud. The algorithm iteratively moves the point cloud differential to solve a predefined multi-demand of geometric properties in gradients, like density. Therefore the process of 'growth' is defined by adding a new point to the point cloud, which is evaluated and executed in repetitive cycles infinitely. These cycles get divided into three operations: (1) grading; (2) relaxing; (3) growing.

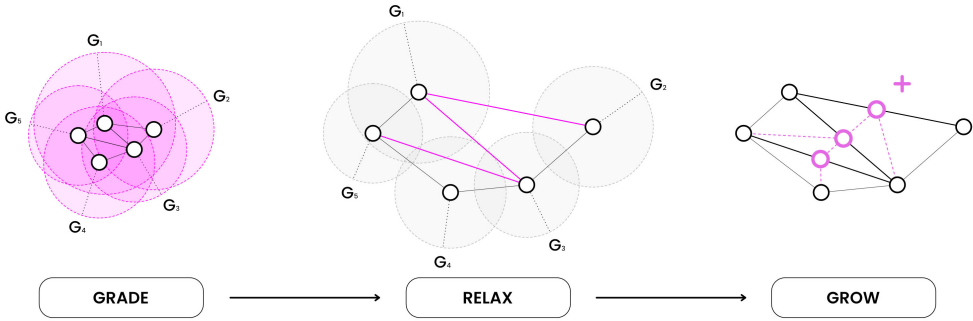


Figure 17: Graded differential growth (GDG): Grade, relax, and grow

- (1) At the beginning of every iteration, the algorithm constructs a new or updated R-Tree, clustering the point cloud (Beckmann et al., 1990). Additionally, each point gets assigned a unique numeric value G , through the multi-demand representative gradient map. G determines the targeted minimum distance to all other points and contributes to the overall movement of the point cloud relaxation. G correlates in this research with the distance between the point itself and the nearest point on the closest stress or boundary curve but could describe any other holistic measurable condition that applies to the entire point cloud.
- (2) Given G for each point, every point's translation vector gets evaluated. The algorithm utilizes the R-Tree for the nearest neighbor search. It accelerates the required local translation vector calculation. Nevertheless, the differing value of G increases or decreases the final translation vector by multiplication. While applied to the points in the point cloud, this undistributed vector transformation causes variable velocities for the point relaxation emerging in differential densities (Figure 18).

The following equations describes the graded relaxation processes in explicit mathematics. Let \hat{p}_1 equal the calculated, updated next point and \hat{p}_0 equal the current point of the point cloud. Let subset $k = \hat{i}_0 \dots \hat{i}_n$ equal the points surrounding the current point \hat{p}_0 for the given radius G and found through the RTree.

Distance between two 3D points:

$$d(\hat{p}, \hat{i}) = \sqrt{(p_x - i_x)^2 + (p_y - i_y)^2 + (p_z - i_z)^2}$$

Graded relaxation of points:

$$\hat{p}_1 = \hat{p}_0 + \frac{\sum_{k=\hat{i}_0}^{\hat{i}_n} 0.5 * (\frac{\hat{p}_0 - \hat{k}}{d(\hat{p}_0, \hat{k})} * (G_0 - d(\hat{p}_0, \hat{k})))}{n}$$

Figure 18: Formula for graded point relaxation

As a result, the overall shape of the cloud gets altered. However, within the relaxation

process, the vector calculation and addition are explicitly executed after another to create a clearly defined cycle. As Menges Nugenyem (2018) described, this separation avoids rapid movements within the point cloud and ensures data structure independent transformations. In comparison, a biased system would evolve following the point chronology of the cloud, translating top-down and causing a shape that originates from that. Furthermore, since every translation vector gets calculated with its nearest neighbors, an unseparated calculation and movement execution would initiate local vector translation anomalies propagating through the entire cloud, affecting already all following calculations and blurring the line between clearly defined cycles.

(3) The point cloud gets organized by defining point pairs. They represent the system on the highest geometric level and are essential for its evolutionary behavior. Each pair length gets calculated by measuring the translation vector from one point to the other. If a pair distance exceeds G of one of the pair's points, it gets classified as relaxed. Subsequently, all relaxed pairs will be divided into two following point pairs, growing the cloud by adding a new point in the middle of the old pair. The iteration starts again.

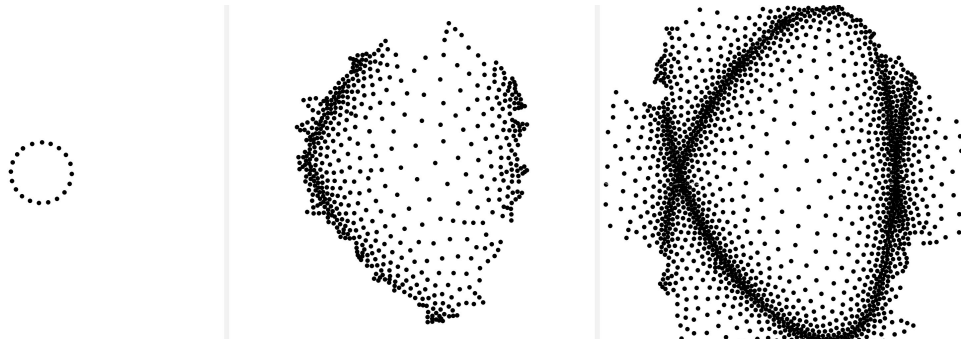


Figure 19: Iterating GDG point cloud, based on a NURBS curve control point structure and an attractor curve grading: left - initial point seed, middle - 150 iterations, right - 300 iterations

Graded differential growth could be applied to any system based on or translatable into vectors of any dimensionality. This research investigates the concept in a three-dimensional geometric context, applying it to control-point based NURBS-curves and vertex-based meshes.

3.3. 3D PRINTING TOOLPATHS: NURBS-CURVE GDG

Modeling and designing bottom up, with the actual material extruded toolpath in AM, is an unconventional design framework, yet it indicates potential for increased printing feasibility, structural performance, and architectural quality if fully controlled (ZHACODE, 2017). The author proposes discretized functionally graded differential curve growth (GDCG) in a 2D to 3D channel for compression-only shells to optimize, constrain, and ultimately utilize a design framework for large-scale AM in architecture. The framework

is based on GDG. A Non-uniform rational basis splines curve (NURBS curve) represents the toolpath in the algorithm. It is a computational geometry structure defining a curve with knots and three-dimensional vectors as control points, which allows geometric transformations of the curve by translating its control points. Therefore the control points of the NURBS curve are the point cloud interface for the GDG.

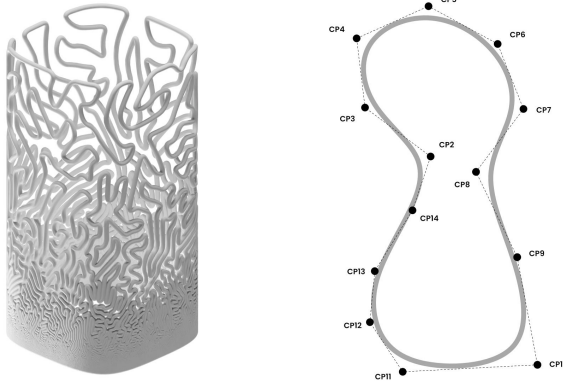


Figure 20: 2D functionally graded differential curve growth by interfacing the control points of a NURBS curve

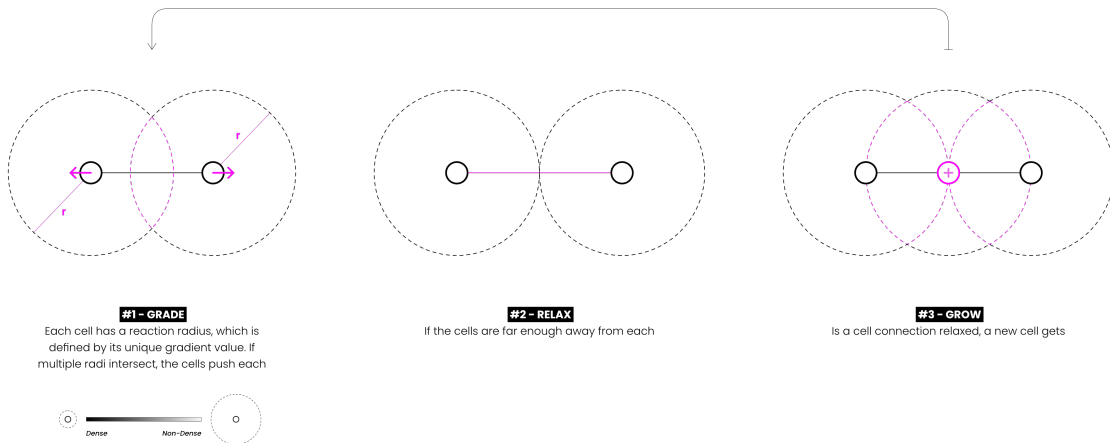


Figure 21: Graded differential curve growth: Grade control points; Relax control points; Grow control points

The design framework for functionally graded toolpaths consists of six steps. (1) The process gets initiated by providing a pre-designed compression-only shell. It represents the key design driver and gets converted into an optimized 3D printing toolpath. (2) The supplied shell gets unrolled, creating a 2D to 3D pipeline through UV translations. (3) With the UV map as a base layer, a multi-demand gets formulated, creating gradients. The gradient gets defined by using, for example, principle stress lines of the shell to spatially divide the UV map into regions of differential structural demands. However, the framework can generate gradient layers with any holistic measurable values of the shell. Furthermore, the UV gradient can be extended with multiple and dynamic updating layers,

ultimately being flexible enough to define sophisticated multi-demands for the toolpath impossible to formulate with a single layer. (4) According to the shell's multi-demand, the toolpath gets grown graded and differential. The framework also discretizes the toolpath for LSAM feasibility into smaller panels to be assembled on-site, taking advantage of in compression working shells. (5) The final grown toolpath panels get printed while supported (subsection 2.1.1) by formwork to ensure the manufacturing of curved profiles. (6) Lastly, the panels get assembled on site.

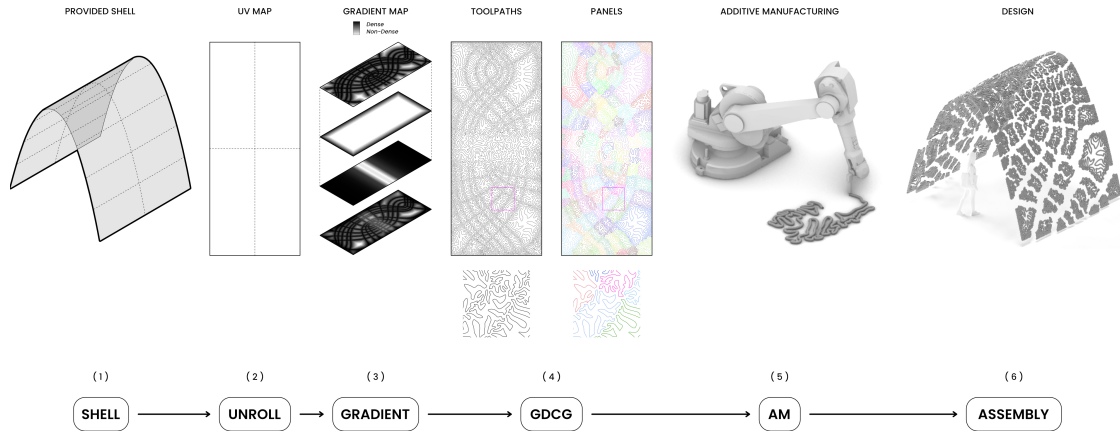


Figure 22: Functionally graded, differential grown, and discretized 3D printing toolpaths framework and applicability to architecture

3.3.1. Developable shells and point cloud seed

The framework is based on compression-only shells to create structurally and AM applicable large-scale geometries, taking advantage of the compression strength of the widespread building material concrete and the force-flow behavior of printing layers, working best in the perpendicular alignment of compression forces. The shell gets unrolled to create a bi-directional mapping flow between its UV coordinates and the global XY plane, defining a 2D to 3D channel. Therefore, the surface and its UV map represent the most significant and form-giving design influence for the grown curve and constitute the framework's main design interface.

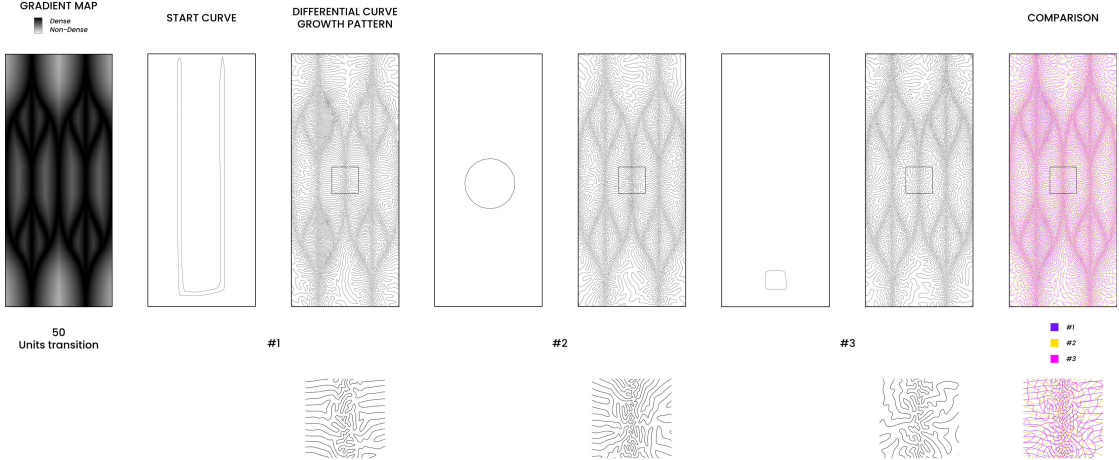


Figure 23: GDCG point cloud seed, represented through a start curve, has deterministic influence on the grown curve

Furthermore, an initial structured point cloud seed for the GDG gets defined through a first NURBS curve, which will evolve and grow. The control-point pairs will determine the connections of the GDG point cloud and the position of new inserted points, consequently contributing to the curve's shape and defining another framework input guiding the growth. For example, figure 23 showcases three point cloud seeds in the same growth condition, developing differential curve patterns. However, the GDG is a deterministic emergent algorithm, and the same initial structured point cloud seed in combination with the same parameters will result in the same growth, which enables the framework to recreate curves fully.

3.3.2. Functional UV gradients

The gradient of the toolpath curve and subsequently the AM design is a gradient of solidity. The curve gradient of the GDG gets achieved by differentially altering the curve control point cloud's local densities. This happens accordingly to a pre-defined or dynamic updating multi-demand, represented by the author through gradient maps, illustrating demanding dense regions in black and demanding loose regions in white. This research investigated three measurable holistic features of the shell to grow functionally graded NURBS curves: (1) distance to principal stress lines/attractor curves; (2) slope; (3) shell boundary.

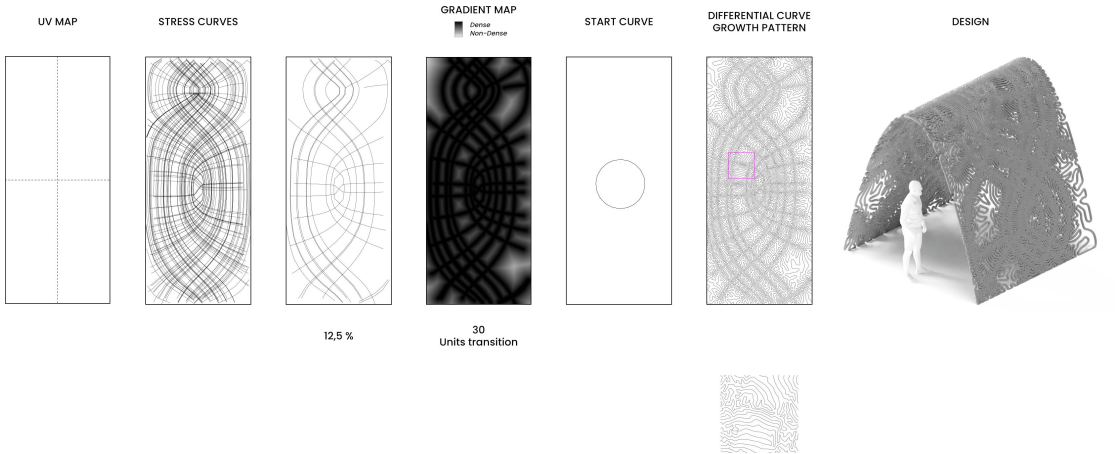


Figure 24: GDCG with principle stress lines of shell geometry

(1) Attractor curves could be rationalized as any curve or line on the UV map. That gives the framework the freedom to incorporate attractors of spatial and artistic quality next to structural relevant attractors. However, in the context of large-scale AM and this research, they represent principle stress lines of the 3D shell unrolled onto the UV map. Given this structural curve network describing compression and tension forces, the gradient gets calculated, defining the distance of every possible location of the unrolled UV map to the closest principle stress curve point among all curves. Simplified, it maps out the principles stress curves proximity on the UV map. It enables a graded reinforcement of structural relevant regions of the shell by solidifying them while eliminating the exposed material in irrelevant structural regions. Nevertheless, since the gradient is based on proximity, the provided attractor curve network must be sparse enough or highly contrasted to create gradients. Therefore, the framework simplifies the principle stress lines by reducing them to 12,5% to filter for regions of significant structural relevance (Figure 24).

- (2) Having a 3D shell, the slope gradient gets calculated and mapped out with the curvature of the UV map.
- (3) To ensure the printability and durability of the architectural design, the boundary edge of the shell gets reinforced by using the outline of the unrolled UV map like an attractor-based gradient, increasing the point cloud's density proportional to its proximity to it.

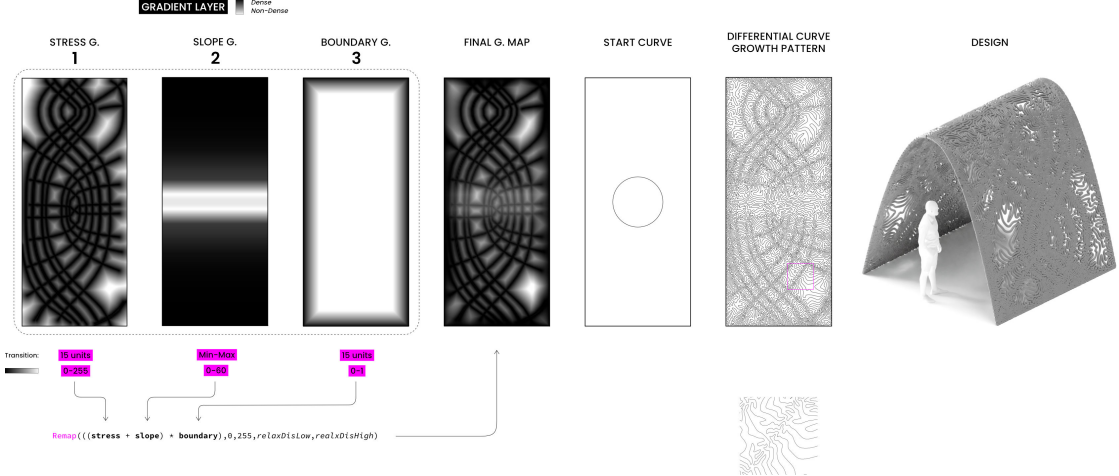


Figure 25: GCG with a multi-layered and weighted gradient defining the unique multi-demand for the shell

The curve design framework also takes advantage of weighted functionally multi-layered grading, combining (1)-(3) into a single, unique gradient map, which represents a higher dimensional multi-demand. Changing the weighting of the gradients or extending the gradient set enables the framework to formulate complex multi-demands to be solved through curve growth (Figure 25).

This research investigated two gradient functions based on attractor curve grading: (1) exponential; (2) linear.

$$f(x) = e^{-x}$$

$$f(x) = mx + b$$

(1) Exponential gradient mapping requires no specific value domain and succeeds with any positive numeric value, consequently giving the framework independence and flexibility. However, because of this infinite gradient, it never reaches the set minimum value, and due to the mathematical nature of an exponential function, peaks in its gradient steps at the very beginning. After a short distance, the gradient values become so proximate that the resulting gradient seems to fade into an almost homogenous area. Indeed, an exponential gradient is characterized by significantly contrasting regions, reducing the actual gradient to a minimum if applied on a large scale (Figure 26 top).

(2) Linear gradient mapping requires an initially defined value domain and works only with numeric values within that domain. Even though this framework is constrained, it gets tailored more explicitly, enabling more control of the created gradient. One example is the adjustable linear blending from domain start and end, resulting in an interface that can fade the contrast (Figure 26 bottom).

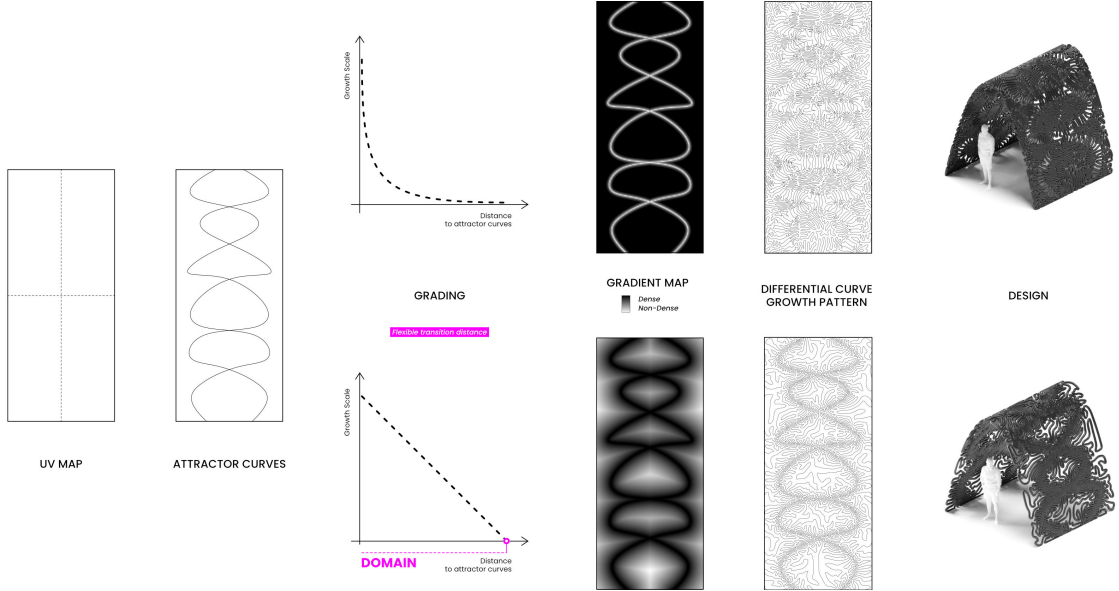


Figure 26: GDCG gradient mapping effect: exponential (top) and linear (bottom)

The two explored gradient functions differed mainly in their resulting contrast intensity, constituting the physical transition distance on the gradient domain while transitioning from start to end. The correlation between the gradient contrast and GDCG got examined in further depth by linearly defining four gradients with differential intensities of contrast by adjusting the gradient domain end (Figure 27).

High contrasting gradients in GDCG, similar to exponential gradients, created curve grains perpendicular to the initial attractor curve and increased the amount of self-intersecting curve anomalies, which contradict the AM feasibility. Furthermore, the grown curve almost replicated the attractors and generated an overall homogeneous pattern with almost no visible gradient in the curve itself (Figure 27 left).

Low contrasting gradients in GDCG formed curve patterns without any geometric anomalies and resulted in visible gradients, emphasizing the heterogeneity of the curve. However, the grain flow and direction of the pattern is more chaotic and not visibly influenced by the initial attractors or anything else (Figure 27 right).

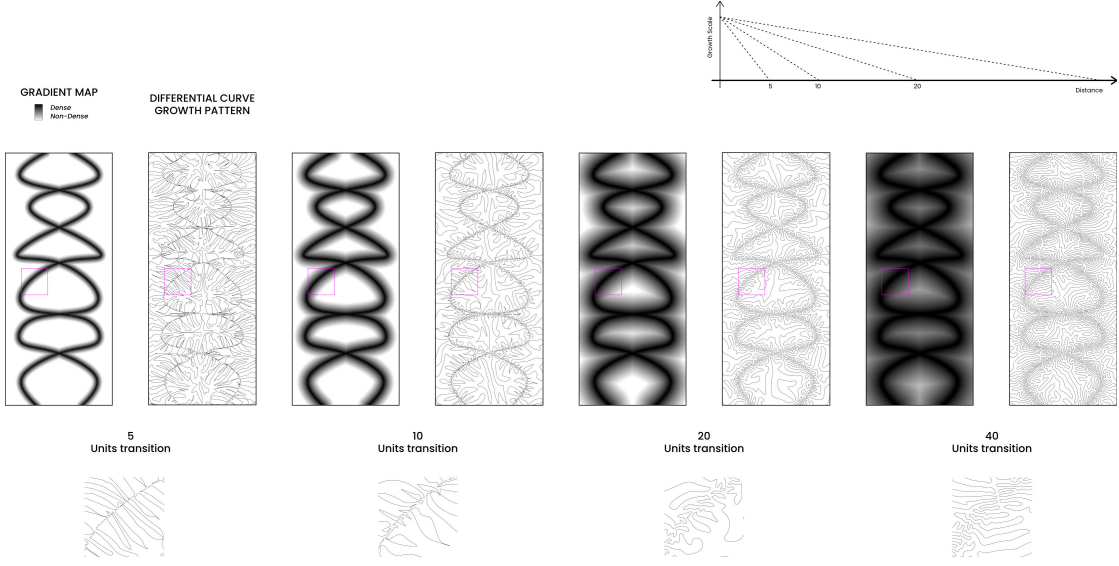


Figure 27: GDCG and the effect of gradient contrast intensities, caused and controlled through the value domain for linear grading.

The gradient contrast analysis showcased more AM feasible and geometric valuable results with low contrasting gradients. However, since the attractor curves only define regions of high demand and a gradient-domain start, the design framework numerically interfaces the gradient domain end, changing the gradient transition distance to control the curve pattern and grain flow for the same multi-demand by blurring or sharpening the contrast.

Dynamic updating gradients, for instance, changing with the GDCG itself got proposed in the context of solidifying panel boundaries in subsection 3.3.4. They opened up a new time and simulation-depending layer to formulate more sophisticated multi-demands within the framework updating over time and impossible with static gradients.

3.3.3. Gradient remapped relaxation

The gradient map constitutes the framework's interface to formulate a multi-demand for the shell to be solved through GDCG. As showcased in the previous chapter (subsection 3.3.2), the gradient contrast significantly contributes to the patterning of the curve by defining the physical transition distance from domain start to end. Further, this domain gets accessed and remapped to a set relaxation distance domain. These relaxation distances are captured through every point's specific and updating value G in GDG and are used to influence the translation of the point cloud. Therefore, the set relaxation distance domain constitutes another control channel for GDCG, increasing or decreasing the relaxation step sizes within the graded point relaxation.

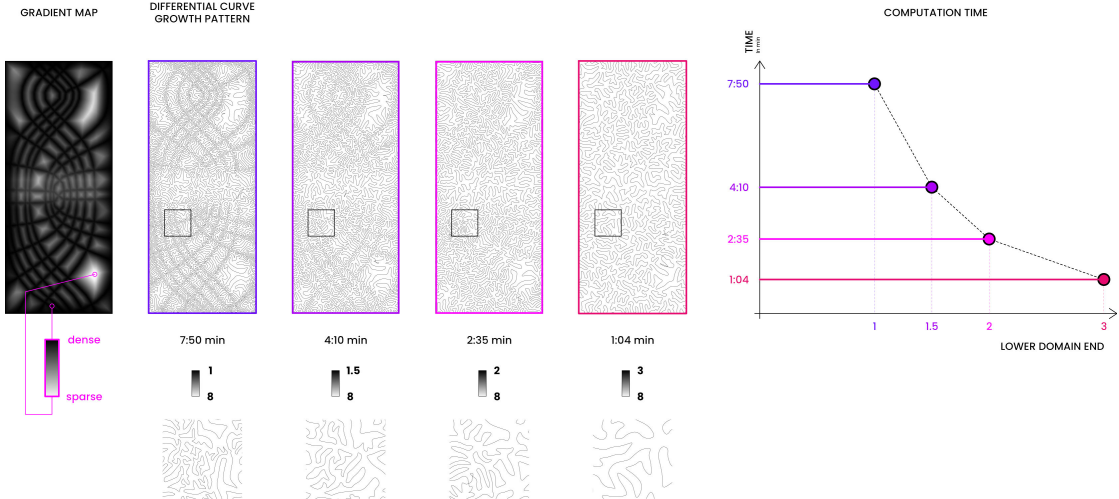


Figure 28: The correlation between the gradient remapped relaxation distance and the resulting curves of GDCG

A study of four prototypes with the identical gradient map was done to analyze the behavior of GDCG by shrinking the gradient remapped relaxation domain (Figure 28). Results show that narrow relaxation domains numerically blur the curve's pattern, creating an almost homogenous toolpath, even though the initial gradient map provides enough contrast. Narrow relaxation domains do not optimize material use through functional toolpaths and are, therefore, less suitable for LSAM.

Increasing or decreasing the relaxation distance domain ultimately influences the growth scales of the point cloud and its resulting total point cloud size. Nearest neighbor search in large point clouds requires much computational power and decelerates the growth process. The conducted GDCG reveals an exponential increase in computation time to grow the curve for the entire UV map by lowering the relaxation domain start and ultimately enlarging the point cloud size. However, the toolpaths with a large remapped relaxation distance domain and high computation time respond the best to the desired multi-demand (Figure 28).

3.3.4. Discretization: Interlocking panels

AM and, in particular, large-scale AM introduce multiple feasibility constraints to be considered in the framework, one of which being the maximum dimensions for designs to get printed at once, caused by the size and amount of axes of the robotic arm. Therefore, the framework explored multiple approaches to discretize the shellular toolpath in printable and efficient panels through multiple, simultaneous graded, differentially grown curves originating from multiple-point clouds structured in an array. However, the aggregation of point clouds is acting as a whole, influencing and moving each other without intersecting. This research examined the following discretization techniques for GDCG: (1) stress grid cell discretizations; (2) evenly distributed, stress-informed discretization; (3) evenly

distributed, diagonally reinforced stress discretization ;(4) panel border reinforced and stress-informed discretization.

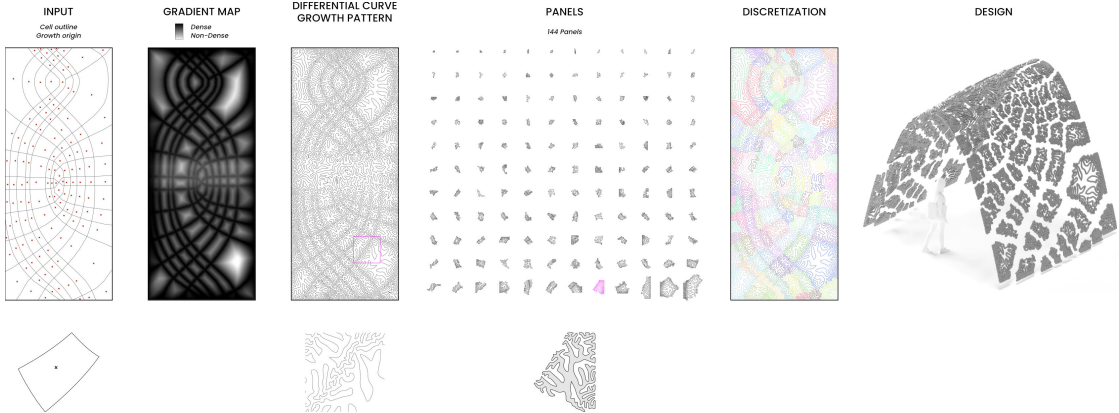


Figure 29: DGDCG through multiple simultaneously grown point clouds, represented through curves, based on principle stress grid cells and informed by a multi-layer gradient.

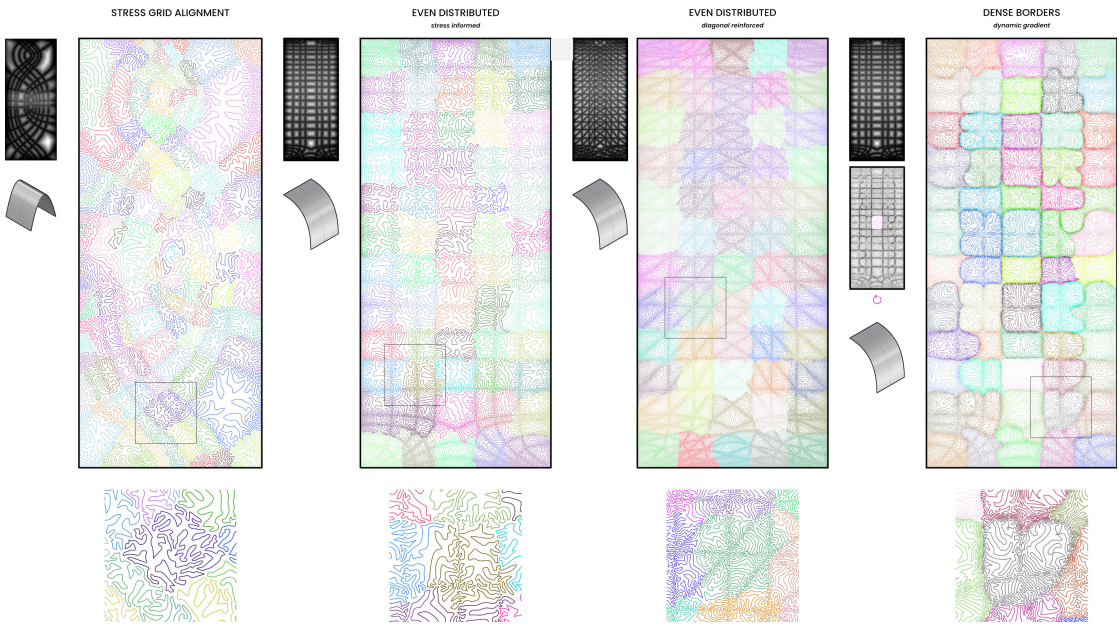


Figure 30: Discretization techniques for GDGCG

(1) The principle stress analysis of the shell geometry creates an irregular grid of compression and tension curves, dividing the shell into stress-informed tiles. These inconsistent stress grid cells got extracted and used for discretizing the AM design and its printed toolpath in a reasonable structural way. For every grid cell, a new initial point cloud was fed to the GDGCG, creating an array of curves growing simultaneously and trying to fulfill the defined multi-demanding gradient map as a whole. The curves themselves were not constrained to their representative grid cell. However, they constituted the varying density and proximity of the stress grid cells resulting in differential competitive growth regions.

(2) The irregularity of the stress grid provokes the emergence of broadly diversified cell sizes, resulting, in approach one, in an increased number of pre-dominantly small tiles

complicating the design assembly. Instead of using the grid cells, approach two feeds an even distributed grid of individual point clouds to the GDCG. The initial point clouds are located independent of the stress grid but grow according to the stress gradient. This generates a tileset with small varieties in panel sizes and avoids significant small or big tiles, simplifying the design's assembly. (3) The approach was adjusted in a third technique to inhibit sparse panel regions constraining the feasibility of AM. The discretization itself is similar to approach two. However, the stress gradient and relaxation domain got extended to reinforce the tiles diagonally and achieve a more solid curve behavior.

(4) This approach introduces dynamic updating multi-demand representing gradient maps. The technique avoids loose printed panels caused by unconstraint panel borders, permitting crack propagation and structural weaknesses during the shell assembly. The multi-layer defined gradient gets extended by another layer, continuously updating itself throughout the GDCG. Every cycle creates with the new array of curves an attractor-based gradient map of those for those, allocating demanding dense regions at the border of the curves and resulting panels. However, to avoid growth singularities, at which the curve is creating a density demanding region for itself, an individual and updated gradient map gets generated for every curve in the array with all other curves except for itself (Figure 31). Nevertheless, over multiple iterations of the GDCG, this approach leads to a solidifying edge between all panels while still mimicking the stress gradient to be structurally feasible and applicable to architecture. However, anomalies are significantly increasing, represented by self-intersecting curves, which challenge the material extrusion and manufacturing of the toolpath.

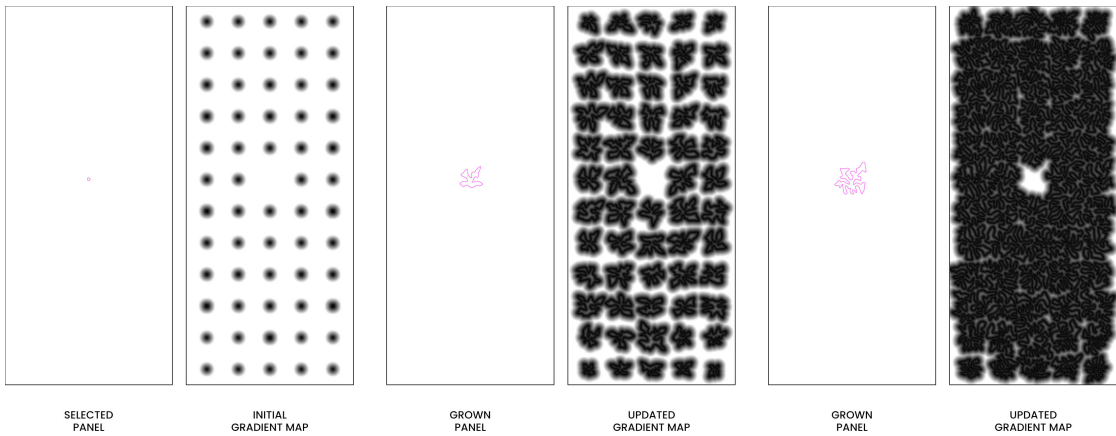


Figure 31: Dynamic gradient that updates every growth iteration accordingly to all other point cloud transformations, creating dense panel borders.

3.4. ARCHITECTURAL SOLIDS: MESH GDG

Functionally graded differential mesh growth (GDMG) is a framework based on GDG for solid geometry datatypes. It investigates the optimization and form generation of multi-demanding solids in architecture. A mesh is a computational geometry structure representing a shape through vertices, which get organized into edges, and solid faces. Simplified, it is a structured point cloud consisting of three-dimensional vertices. This fundamental geometric feature makes a mesh applicable to the GDG algorithm, interfacing and growing the vertex cloud, which ultimately alters its edges, faces, and compositional shape.

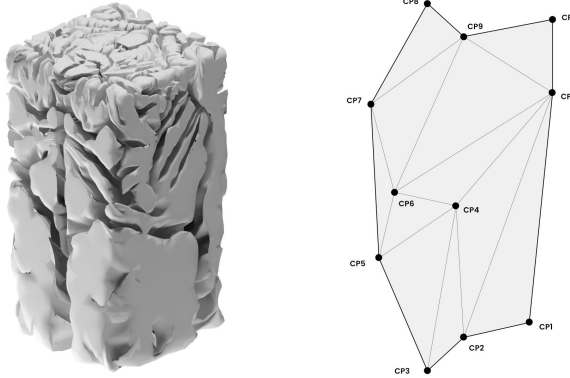


Figure 32: 3D graded differential mesh growth by interfacing the vertices of a mesh

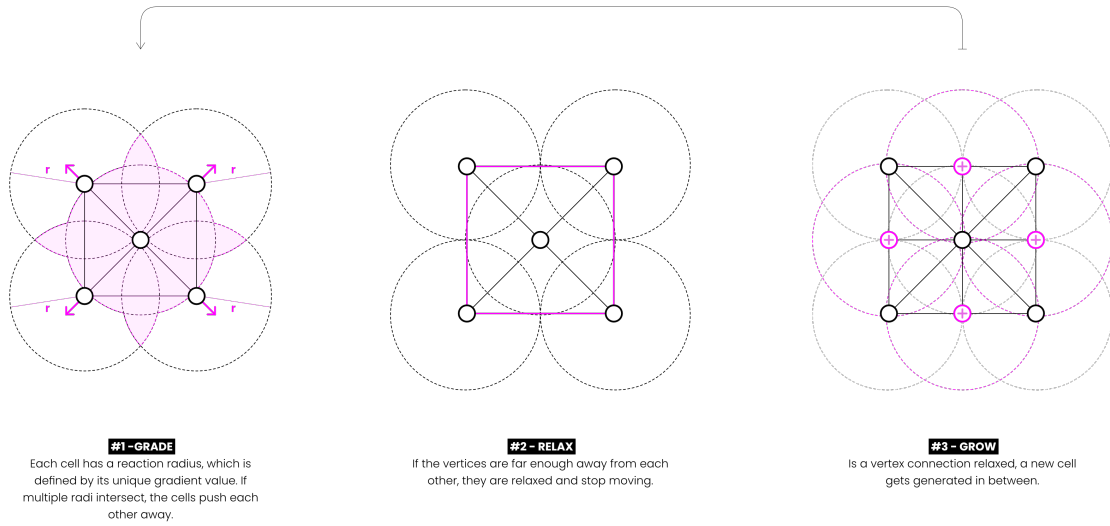


Figure 33: Graded differential mesh growth: Grade vertices; Relax vertices; Grow vertices

The GDMG framework represents a second use case for GDG in architecture. However, it was not studied in full depth and proposes a similar framework as GDCG (section 3.3) to explore graded grown meshes.

The framework consists of four steps: (1) An initial, solid design representation in the form of a BRep needs to be provided, defining the 3D volume to form-find and constraining the growth. The boundary shape is the virtual interface of the GDMG and enables the graded mesh growth for explicit design contexts and forms. (2) A 3D gradient gets calculated and defined with attractors or other holistic measurable information for the whole boundary shape, differentiating the local regions of the 3D volume and formulating the multi-demand. (3) A point cloud seed gets set by providing a low-resolution start mesh, representing the origin of the growth. (4) The mesh grows over multiple iterations the vertex cloud, resulting in a graded, complex folded mesh fulfilling the multi-demand.

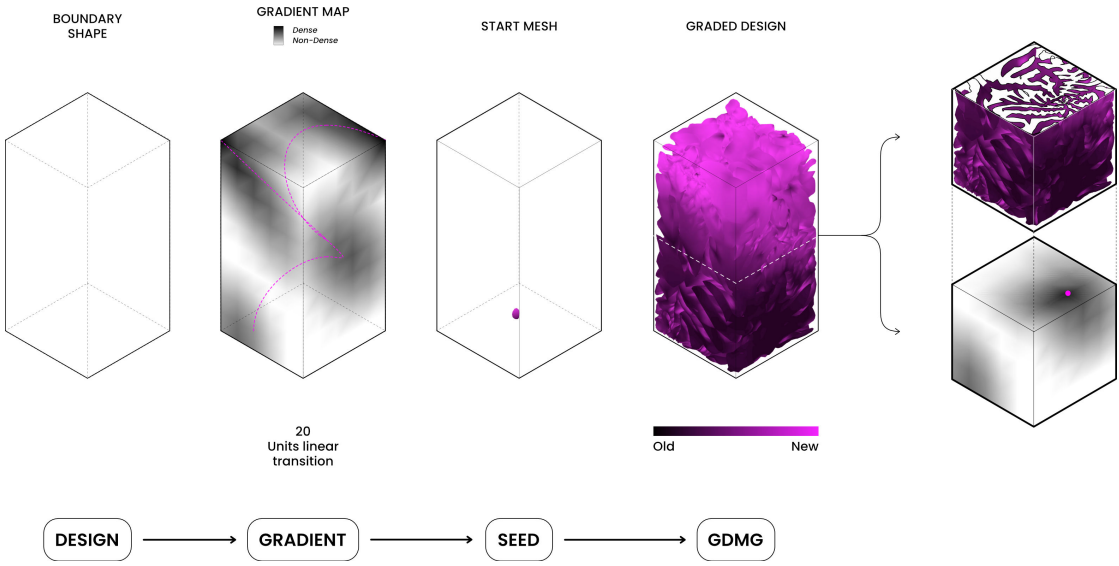


Figure 34: Graded differential mesh growth framework

3.4.1. Boundary shapes and functional 3D gradients

The provided boundary representative shape is the most significant interface of the GDMG and creates its compositional design. This BRep conversion channel enables the framework to create specific, optimized shapes rather than random mesh emergence. The constraint is implemented by decelerating the point cloud relaxation exponentially to the distance of the boundary design. That causes the vertices to reach a movement singularity towards the boundary, eventually forcing them to stop moving, hitting a specified threshold. Consequently, this process divides the point cloud into regions with differential growth speeds and only allows particular areas to continue growing within the initial shape. The framework separates between new and old areas of the mesh, representing the time chronology of the mesh from black, old, to new, magenta (Figure 35).



Figure 35: Architectural application of GDMG: Furniture (left), Pavilion (right)

The 3D gradient for the GDMG uses the gradient design framework of GDCG. A 3D multi-demand is formulated through attractor curves (subsection 3.3.2).

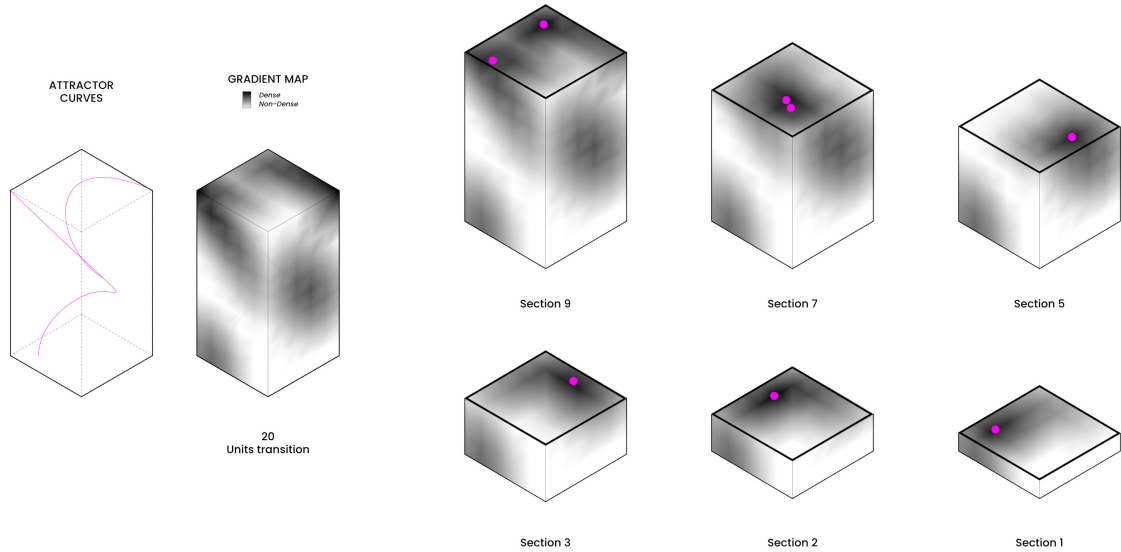


Figure 36: 3D gradients through attractor curves for GDMG

4. EVALUATION

The outlined algorithm for graded differential growth (section 3.2) proves the potential for solid geometry modeling and advanced toolpath design to create high-performance geometries out of base geometries through graded point relaxation. Prototypes for a column were created using graded differential mesh growth (GDMG)(section 3.4) and graded differential curve growth (GDCG)(section 3.3)(Figure 37). Results validate mass reduction to up to 97% of architectural components compared to their conventional solid counterparts while responding to the structural multi-demand through density gradients.

For GDCG, a pre-modeled shell was provided to the algorithm with a multi-layered gradient utilizing the shells slope, boundary, and principal stress lines to formulate a functional multi-demand (subsection 3.3.2). The toolpath representative curve was initiated and discretized following an even panel distribution (subsection 3.3.4). The resulting LSAM toolpath design diminishes 97% of its solid and 22% of its thin-shell geometric counterpart.

For GDMG, a pre-modeled boundary representation (BRep) of a column was used in combination with a z-axis-based 3D gradient to form-find an optimized geometry of the provided design (section 3.4). The result utilizes 48% of the BReps volume and increases its geometric details and branching scale in a tree-like shape from bottom to top.

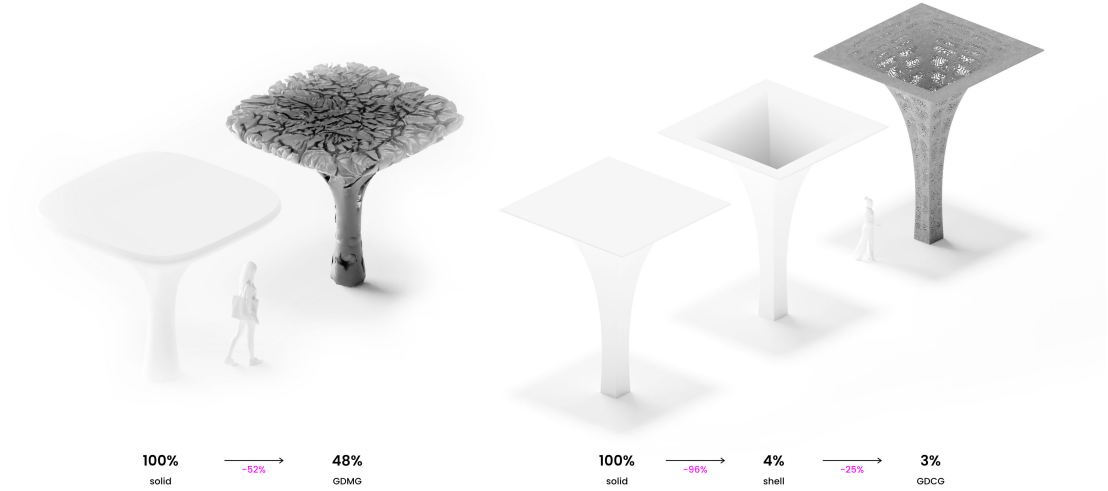


Figure 37: Comparison: Material reduction through GDMG (left) and GDCG (right)

4.1. CONTRIBUTION AND DISCUSSION

Both prototypes fully mimic their boundary representation and showcase the design conversion workflow in an architectural context to be considered the framework’s general design interface. The design optimization pipeline entirely depends on the provided

geometry and its formulated multi-demand in the form of a gradient and facilitates the integration of GDG in conventional design workflows. It heavily relies on its user and enables controlled design diversity within the same computational framework.

The results of GDMG and GDCG demonstrate the potential of both techniques to optimize geometries for decreased and more efficient material use. However, GDCG reveals significantly more relevance in light of recent research, challenges, and sustainable qualities in LSAM and FGD in architecture. GDCG bridges LSAM and FGD to overcome both of their CAD constraints (subsection 2.3.1), thus, enabling the utilization of AM broadly in architecture to lower carbon emissions of the AEC industry. GDCG contributes to a sustainable design paradigm in architecture driven by extrusion-based AM and constitutes a facilitated design framework for 3D printing in architecture by diminishing building material up to 22%, taking full advantage of the manufacturing tectonics. The entire framework is based on geometry modeling, material deployment, and building materials with high compression strength due to the widespread use of concrete and the brick-masonry-like behavior of unreinforced 3D printing layers (Bhooshan et al., 2018b).

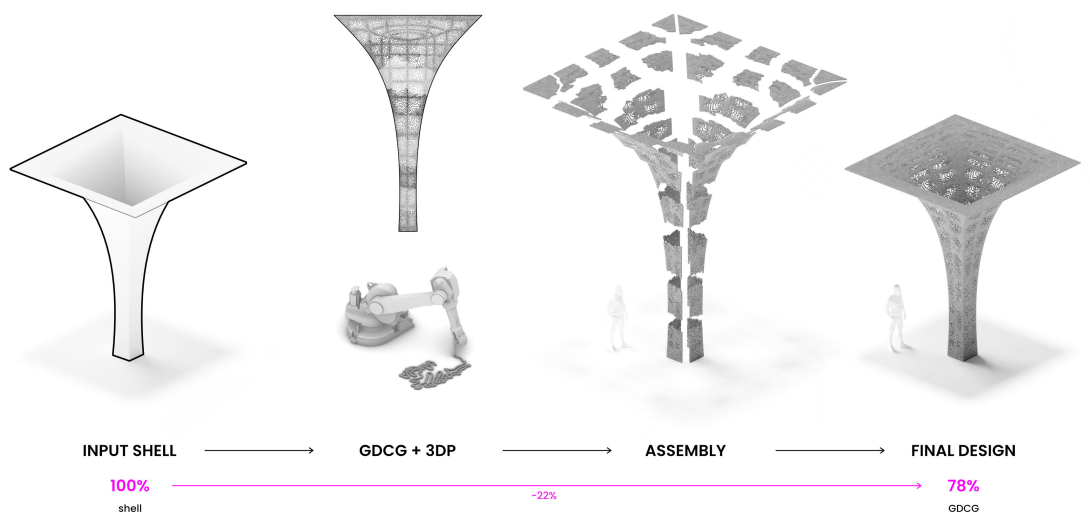


Figure 38: DGDG framework for a new, sustainable architecture language enabled through LSAM and FGD

The synthesized lack of explicit design software for LSAM (Bhooshan et al., 2018a), decelerating the take-off of AM in architecture, and the lack of modeling software for FGD (Hasanov et al., 2022; Oxman et al., 2011), blocking the efficient use of building material, got recognized and approached by developing a design framework contributing and fulfilling both domain gaps for a greener design language in architecture. Moreover, the design framework is highly flexible and automated, creating toolpath designs for provided shapes and multi-demands while reducing costs and construction time with

minimal prior knowledge. Additionally, AM enables the usage of local materials like clay or soil and only requires a robotic printer, whereas other construction techniques for example out of timber, depend on expensive machinery and specific environments. The facilitated appliance is significantly relevant to low-income countries representing global urbanization centers that depend heavily on cheap, fast, and low-tech architectural solutions like GDCG for functionally graded AM.

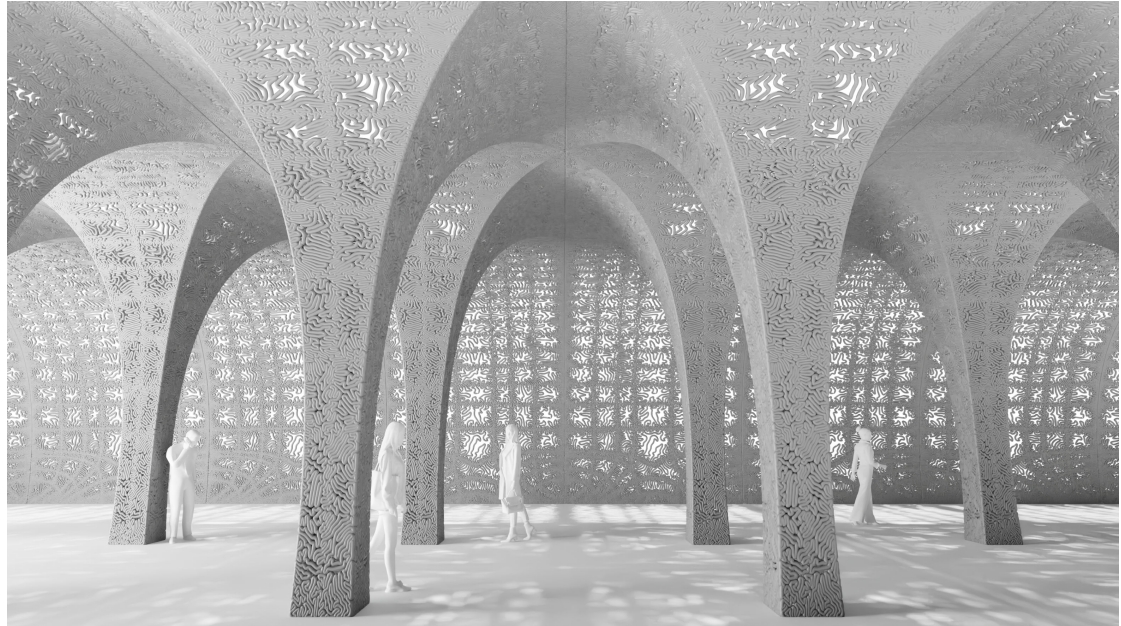


Figure 39: Concept rendering: functionally graded 3D printing toolpaths in architecture

4.2. FUTURE WORK

Functionally graded 3D printing toolpaths have been rarely researched, yet they show potential to optimize AM further and contribute to a unique design paradigm shaped by and impossible without 3D printing. Further investigation of the intersection of FGD and AM is necessary.

4.2.1. Functionally graded 3D printing toolpaths

The presented design framework requires large-scale prototypes to get tested and evaluated for ultimate architectural applicability. Specifically, studies with relevant architectural and compressive materials like concrete are required to assess functionally graded toolpaths for LSAM.

New mathematical concepts for GDG improving the transformation of large structured point clouds should be explored to enable high-resolution toolpath detailing without

significantly increased computation time (subsection 3.3.3).

However, the current design framework limits itself to the outlined algorithm for graded differential growth, contributing significantly to the resulting toolpath's overall shape and behavior. Functionally graded 3D toolpaths constitute a promising sub-domain within the field of AM, especially LSAM. Additional studies should be done approaching those with new concepts.

Further, algorithmic tailoring for explicit and robot-depending constraints has to be done, extending GDCG to incorporate additional forces in the toolpath growth to ensure printing feasibility. The full potential of GDCG for toolpaths has yet to be discovered by increasing the multi-demanding matrix with other channels driving the toolpath growth.

The current framework is based on curve-like shapes creating toolpaths with limited control of their direction or alignment next to the gradient contrast and initial point cloud seed, provided through a set gradient transition distance and start curve. The direction of the toolpath grains in the pattern is relevant for the compression flows within the shell and shows potential to be controlled further, enhancing structural performance and unlocking thinner panels to reduce material. Additionally, these intentionally directed grains could be reinforced with fibers during the 3DP manufacturing process. However, the behavior and optimization of these printed grain structures need to get investigated further from a computational, material, and structural standpoint.

4.2.2. Graded differential growth

However, besides the dominant focus on functionally graded toolpaths, GDG needs more research with other geometries to unveil potentials in new contexts.

Utilizing the GDG for printing infills in AM could be relevant and needs exploration. It represents an easy interface to generate functionally graded geometric profiles for extrusions and solids in current design environments and would enhance the use of FGD.

It requires further analysis of the correlation and applicability between GDG and other AM technologies, like powder-based AM and binder-jetting. With that, the 3D interlocking behavior of GDMG could be studied and used for advanced discretizing.

5. CONCLUSION

5.1. RESEARCH SUMMARY

Additive manufacturing (AM) and functionally graded design (FGD) represent historical, interdisciplinary design and manufacturing techniques that receive ever-increasing attention in architecture to achieve sustainability, mass customization, and construction acceleration for global urbanization. As stated in the introduction, it is required to facilitate the digital incorporation of these in the architectural industry (chapter 1).

Contemporary large-scale additive manufacturing (LSAM) in architecture was analyzed, presenting state-of-the-art toolpath design principles (section 2.1) through groundbreaking projects like the striatus bridge (ZHACODE et al., 2021) and the thallus installation (ZHACODE, 2017). Furthermore, functionally graded design (FGD) got introduced and explained by means of architectural precedents like the durotaxis chair (SynthesisDesign+Architecture and Stratasys, 2014) and the aguahoja pavillion (Duro-Royo et al., 2018). The author divided the domain of FGD into functionally graded materials (FGMs) and functionally graded geometries (FGGs), differing material quantity and recyclability (section 2.2). Finally, historic architectural design frameworks got presented and examined along with their task of unifying research and practice to create innovation in construction. Ultimately, the design lack of computer-aided design (CAD) for LSAM and FGD got unveiled and examined with recent software solutions for it (section 2.3).

An algorithm for graded differential growth (GDG) got outlined, deterministically and iteratively creating graded point clouds (section 3.2). The algorithm got extended and further investigated with graded differential curve growth (GDCG), showcasing the novel technique of generating functionally graded toolpaths for extrusion-based AM. It created a facilitated design framework for AM in architecture by cross-connecting FGD, as a modeling technique, and LSAM, as a manufacturing method (section 3.3). Additional studies with GDG in the context of solid geometry modeling were done, exploring functionally graded differential mesh growth (GDMG)(section 3.4).

Architectural prototypes with GDMG and GDCG were analyzed, indicating significant mass loss by reducing conventional, solid architectural components up to 3%. The relevance and contribution of GDCG in the context of facilitated toolpath design frameworks in architecture was outlined, discussed, and analyzed for future work.

5.2. CONCLUSION

A computational design framework to functionally grade toolpaths for extrusion-based large-scale additive manufacturing got outlined. It aims to extend contemporary CAD software and bypass its revealed modeling constraints for functionally graded design (FGD) and large-scale additive manufacturing (LSAM) to contribute to a more ecological and economical architectural design paradigm. The framework combines, for the first time, functionally graded geometries (FGGs) and LSMA to introduce a new, sustainable tectonism in architecture driven by 3D printing. It utilizes the research's presented algorithm for graded differential growth (GDG) to create functionally graded 3D toolpaths for compression-only shells, elaborating a facilitated toolpath design optimization framework to fulfill the globally, ever-accelerating urbanization with LSAM. The workflow bridges the gap between design and manufacturing by form-finding toolpaths according to the topology of pre-defined shells. Single layered, multi-layered and dynamic updating gradient maps get explored and analyzed for formulating complex multi-demands of shells to be solved through FGGs. Additionally, stress-aligned, distributed, and dynamic discretization techniques get investigated to divide large toolpath designs into smaller, printable panels, incorporating the dimension limitations of robotic printing. The framework entirely abandons conventional, planar slicing of geometries for AM as well as LSAM and provides an unprecedented, facilitative control channel for creating toolpaths, following a bottom-up approach. The toolpath representing NURBS curve gets iteratively form-found to fulfill the desired multi-demand. The design framework constitutes a novelty for advanced toolpath creation due to its flexible optimization process, synthesizing uniquely tailored toolpaths for custom-provided demands and shells. Results proved the potential to significantly diminish material by reducing conventional solid shells up to 22% of their original mass.

The dissertation demonstrated the potential and novelty of graded, high-performance, and sustainable architectural geometry only feasible through additive manufacturing and functionally graded design by introducing a new design language in architecture, a new tectonism.

BIBLIOGRAPHY

- AiBuild. Aisync. *AiBuild*, 2022. URL <https://ai-build.com>.
- A. Anton, A. Yoo, P. Bedarf, L. Reiter, T. Wangler, and B. Dillenburger. Vertical modulations: Computational design for concrete 3d printed columns. 10 2019. doi: 10.52842/conf.acadia.2019.596.
- L. Barcelo, J. Kline, G. Walenta, and E. Gartner. Cement and carbon emissions. *Materials and Structures/Materiaux et Constructions*, 47:1055–1065, 2014. ISSN 13595997. doi: 10.1617/s11527-013-0114-5.
- N. Beckmann, H.-P. Kriegel, R. Schneider, and B. Seeger. The r*-tree: An efficient and robust access method for points and rectangles. In *Proceedings of the 1990 ACM SIGMOD international conference on Management of data*, pages 322–331, 1990.
- M. P. Bendsøe and N. Kikuchi. Generating optimal topologies in structural design using a homogenization method. *Computer Methods in Applied Mechanics and Engineering*, 71:197–224, 1988. ISSN 0045-7825. doi: [https://doi.org/10.1016/0045-7825\(88\)90086-2](https://doi.org/10.1016/0045-7825(88)90086-2). URL <https://www.sciencedirect.com/science/article/pii/0045782588900862>.
- S. Bhooshan, J. Ladinig, T. Van Mele, and P. Block. Function representation for robotic 3d printed concrete. In *Robotic Fabrication in Architecture, Art and Design 2018*, pages 98–109. Springer International Publishing, Cham, 2018a. ISBN 3319922939.
- S. Bhooshan, T. V. Mele, and P. Block. Equilibrium-aware shape design for concrete printing, 2018b.
- I. Campbell, O. Diegel, J. Kowen, and T. Wohlers. Wohlers report 2017 3d printing and additive manufacturing state of the industry: Annual worldwide progress report, 2017.
- S. S. Crump. Apparatus and method for creating three-dimensional objects, June 9 1992. US Patent 5,121,329.
- R. Dawkins. *The blind watchmaker*. Penguin, repr. with appendix. edition, 1991. ISBN 0140144811.
- C. T. de Mello Soares, M. Ek, E. Östmark, M. Gällstedt, and S. Karlsson. Recycling of multi-material multilayer plastic packaging: Current trends and future scenarios. *Resources, Conservation and Recycling*, 176, 1 2022. ISSN 18790658. doi: 10.1016/j.resconrec.2021.105905.
- A. Dolenc and I. Mäkelä. Slicing procedures for layered manufacturing techniques. *Computer-Aided Design*, 26(2):119–126, 1994. ISSN 0010-4485. doi: [https://doi.org/10.1016/0010-4485\(94\)90032-9](https://doi.org/10.1016/0010-4485(94)90032-9). URL <https://www.sciencedirect.com/science/article/pii/0010448594900329>.
- J. Duro-Royo, J. V. Zak, A. Ling, Y.-J. Tai, N. Hogan, B. Darweesh, and N. Oxman. Designing a tree: Fabrication informed digital design and fabrication of hierarchical structures. volume 2018, pages 1–7, 2018.
- L. J. Gibson and M. F. Ashby. *Cellular Solids: Structure and Properties*. Cambridge solid state science series. Cambridge University Press, 1997. ISBN 9780521499118.
- A. Gupta and M. Talha. Recent development in modeling and analysis of functionally graded materials and structures. *Progress in Aerospace Sciences*, 79:1–14, 2015. ISSN 03760421. doi: 10.1016/j.paerosci.2015.07.001.

- E. Haeckel. *Art Forms in Nature*. 1899.
- S. Hasanov, S. Alkunte, M. Rajeshirke, A. Gupta, O. Huseynov, I. Fidan, F. Alifui-Segbaya, and A. Rennie. Review on additive manufacturing of multi-material parts: Progress and challenges. *Journal of Manufacturing and Materials Processing*, 6, 2022. ISSN 2504-4494. doi: 10.3390/jmmp6010004. URL <https://www.mdpi.com/2504-4494/6/1/4>.
- C. Huang, Z. Wang, D. Quinn, S. Suresh, and K. J. Hsia. Differential growth and shape formation in plant organs. *Proceedings of the National Academy of Sciences of the United States of America*, 115: 12359–12364, 12 2018. ISSN 10916490. doi: 10.1073/pnas.1811296115.
- C. W. Hull. Apparatus for production of three-dimensional objects by stereolithography. *United States Patent, Appl., No. 638905, Filed*, 1984.
- F. IGD. Cad-modelle gradieren – elegant, funktional und intuitiv. *Frauenhofer-Institut für Graphische Datenverarbeitung IGD*, Mar 2021. URL <https://www.igd.fraunhofer.de/de/media-center/presse/cad-modelle-gradieren---elegant--funktional-und-intuitiv-.html>.
- A. Kawasaki and R. Watanabe. Concept and p/m fabrication of functionally gradient materials, 1997.
- J. Klein, M. Stern, M. Kayser, C. Inamura, G. Franchin, S. Dave, D. Lizardo, P. Houk, and N. Oxman. Glass i, 2015. URL <https://oxman.com/projects/glass-i>.
- R. Korner. Fraunhofer igd ermöglicht mit software „grammacad“ die modellierung graderter 3d-objekte. *3D-grenzenlos Magazin*, Oct 2020. URL <https://www.3d-grenzenlos.de/magazin/3d-software/grammacad-3d-objekte-mit-gradierten-eigenschaften-modellieren-27623353/>.
- M. Leinster. Things pass by. *Thrilling Wonder Stories*, 1945.
- R. M. Mahamood, E. T. Akinlabi, M. Shukla, and S. L. Pityana. Functionally graded material: an overview. 2012.
- R. Mehl. Der urahn des betondrucks: Die urschel wall building machine. *Baublatt*, Oct 2021. URL <https://www.baublatt.ch/baupraxis/der-urahn-des-betondrucks-die-urschel-wall-building-machine-31788>.
- A. Menges and L. Nguyen. Workshop live-streaming: C# scripting and plugin development for grasshopper, April 2018. URL <https://www.icd.uni-stuttgart.de/teaching/workshops/workshop-live-streaming-c-scripting-and-plugin-development-for-grasshopper/>.
- W. J. Mitchell. A new agenda for computer-aided design. 1990.
- D. Mitterberger and T. Derme. Digital soil: Robotically 3d-printed granular bio-composites. *International Journal of Architectural Computing*, 18(2):194–211, 2020.
- O. A. Mohamed, S. H. Masood, and J. L. Bhowmik. Experimental and statistical modeling on surface roughness for fdm pc-abs polymeric material using d-optimal design. In M. Hashmi, editor, *Encyclopedia of Materials: Plastics and Polymers*, pages 271–278. Elsevier, Oxford, 2022. ISBN 978-0-12-823291-0. doi: <https://doi.org/10.1016/B978-0-12-820352-1.00103-6>. URL <https://www.sciencedirect.com/science/article/pii/B9780128203521001036>.
- N. Müller and J. Harnisch. A blueprint for a climate friendly cement industry. *Gland: WWF Lafarge conservation partnership*, 2008.

- MX3D. Mx3d bridge, 2021. URL <https://mx3d.com/industries/infrastructure/mx3d-bridge/>.
- T. D. Ngo, A. Kashani, G. Imbalzano, K. T. Nguyen, and D. Hui. Additive manufacturing (3d printing): A review of materials, methods, applications and challenges, 6 2018. ISSN 13598368.
- H. Niknam and A. H. Akbarzadeh. Thermo-mechanical bending of architected functionally graded cellular beams. *Composites Part B: Engineering*, 174:107060, 6 2019. doi: 10.1016/j.compositesb.2019.107060.
- E. Obataya, P. Kitin, and H. Yamauchi. Bending characteristics of bamboo (*phyllostachys pubescens*) with respect to its fiber-foam composite structure, 6 2007. ISSN 00437719.
- N. Oxman, S. Keating, and E. Tsai. Functionally graded rapid prototyping, 6 2011.
- G. Poleni and J. Poleni. *Memorie Istoriche Della Gran Cypola Del Tempio Vaticano, E De'Danni Di Essa, E De'Ristoramenti Loro, Divise In Libri Cinque*. Nella Stamperia del seminario, 1748.
- prostep ivip Association. Additive manufacturing interfaces. 2021.
- P. Prusinkiewicz and A. Lindenmayer. *The algorithmic beauty of plants*. 1990.
- M. Rippmann and P. Block. Rethinking structural masonry: Unreinforced, stone-cut shells. *Proceedings of the ICE - Construction Materials*, 166(6):378–389, 2013. doi: 10.1680/coma.12.00033.
- J. Rosenkrantz and J. Louis-Rosenberg. Growing objects. *Nervous System*, 2014. URL <https://n-e-r-v-o-u-s.com/projects/albums/growing-objects/>.
- A. Scholzen, R. Chudoba, and J. Hegger. Thin-walled shell structures made of textile-reinforced concrete: Part i: Structural design and construction. *Structural Concrete*, 16:106–114, 3 2015. ISSN 17517648. doi: 10.1002/suco.201300071.
- P. Schumacher. Tectonism in architecture, design and fashion: Innovations in digital fabrication as stylistic drivers. *Architectural Design*, 87(6):106–113, 2017.
- Y. Shinohara. Chapter 11.2.4 - functionally graded materials, 2013. URL <https://www.sciencedirect.com/science/article/pii/B9780123854698000617>.
- F. Simancik. Reproducibility of aluminium foam properties. *Metal Foams and Porous Metal Structures*, 01 1999.
- P. S. Stevens. *Patterns in Nature*. Little, Brown, 1974. ISBN 9780316813280. URL <https://books.google.co.uk/books?id=LQynQgAACAAJ>.
- SynthesisDesign+Architecture and Stratasys. Durotaxis chair, 2014. URL <https://www.synthesis-dna.com/portfolio/durotaxis-chair/>.
- G. Tang. An overview of historical and contemporary concrete shells, their construction and factors in their general disappearance, 2015.
- D. W. Thompson. *On growth and form / by D'Arcy Wentworth Thompson*. University Press, 1917.
- United Nations, Department of Economic and Social Affairs, Population Division. 2022 world population prospects 2022: Ten key messages, 2022. URL https://www.un.org/development/desa/www.un.org.development.desa.pd/files/wpp2022_summary_of_results.pdf.

United Nations Environment Programme. 2021 global status report for buildings and construction: Towards a zero-emission, efficient and resilient buildings and construction sector, 2021. URL <https://globalabc.org/resources/publications/2021-global-status-report-buildings-and-construction>.

W. E. Urschel. Machine for building walls. *USA Patent US2339892A*, 1944.

T. Wangler, E. Lloret, L. Reiter, N. Hack, F. Gramazio, M. Kohler, M. Bernhard, B. Dillenburger, J. Buchli, N. Roussel, et al. Digital concrete: opportunities and challenges. *RILEM Technical Letters*, 1:67–75, 2016.

J. Wolff. *The law of bone remodelling*. Springer Science & Business Media, 2012.

R. Wolfs, F. Bos, and T. Salet. Hardened properties of 3d printed concrete: The influence of process parameters on interlayer adhesion. *Cement and Concrete Research*, 119:132–140, 2019. ISSN 0008-8846. doi: <https://doi.org/10.1016/j.cemconres.2019.02.017>. URL <https://www.sciencedirect.com/science/article/pii/S0008884618310482>.

K. V. Wong and A. Hernandez. A review of additive manufacturing. *ISRN Mechanical Engineering*, 2012: 1–10, 8 2012. doi: 10.5402/2012/208760.

N. Yunis and K. Watkins. Frei otto and the importance of experimentation in architecture. *arch daily*, Mar 2015. URL <https://www.archdaily.com/610531/frei-otto-and-the-importance-of-experimentation-in-architecture>.

ZHACODE. Thallus installation, 2017. URL <https://www.zaha-hadid.com/design/thallus-installation/>.

ZHACODE, BRG, incremental3D, and Holcim. Striatus 3d concrete printed masonry, 2021. URL <https://www.striatusbridge.com>.